Isotropic magnetic shielding in the classification of aromaticities for low-lying electronic states of benzene and cyclobutadiene with an additional investigation into non-orthogonal Boys localization

Peter Hearnshaw

MSc by Research

University of York

Chemistry

December 2016

Abstract

Quantum chemical calculations are performed to analyse the isotropic shielding over a fine grid through benzene and cyclobutadiene in various electronic states in order to analyse aromaticity. The use of both two-dimensional contour plots and three-dimensional isovalue plots allows unambiguous classification of aromaticity and antiaromaticity. The S_0 and S_2 states of benzene and the S_1 and T_1 states of cyclobutadiene are found to be aromatic whilst the S_1 and T_1 states of benzene and the S_0 and S_2 states of cyclobutadiene are found to be antiaromatic. This was found to be in agreement with previous predictions based on NICSs and magnetic susceptibility exaltations, but the current method was able to provide a far clearer distinction between the aromatic and antiaromatic states. Furthermore a study was performed to investigate the possibility of a non-orthogonal Boys localization procedure. Taking the molecular orbitals of water as an example, an algorithm was implemented which scanned a vast number of transformation matrices in an attempt to minimize the Boys functional with no constraint on orthogonality. It was found that the value of the Boys functional could be increased by removal of the orthogonality constraint but that critical problems arose concerning orbitals becoming linearly dependent. Methods of solving the self-convergence problem for non-orthogonal localized orbitals are suggested including the use of an alternative localization functional.

Contents

List of Figures

List of Tables

Acknowledgements

I would like to thank Dr Peter Karadakov for teaching in all matters related to quantum chemistry along with support and guidance throughout the masters year. Dr Kate Horner for support in how to implement the calculations. Josh Kirsopp for thought-provoking conversations in all manner of topics relating to science and maths. William Drysdale for discussions about programming and the fundamentals of quantum mechanics. And the other members of the Karadakov group, Muntadar and Make, for their company and support.

I also owe a great deal of thanks to Hannah Harris, Clare Hearnshaw and Jennifer Hearnshaw for encouragement and support. Lastly to the Department of Chemistry at the University of York who have given me what I needed to complete the research.

Declaration

I declare that this thesis is a presentation of original work and I am the sole author. This work has not previously been presented for an award at this, or any other, University. All sources are acknowledged as References. A journal article has been published using work produced in this thesis, see Ref [5].

1 Quantum chemical theory

1.1 The development of quantum chemistry

Quantum chemistry, the study of electronic structure of molecules, is one of the most important and intriging problems to which quantum mechanics can be applied. The theory of quantum mechanics describes the behaviour of particularly small objects and was developed at the first half of the 20th century. It became clear that this new theory could be of great importance to chemistry, so much so that leading physicist Paul Dirac famously said "the fundamental laws necessary for the mathematical treatment of a large part of physics and the whole of chemistry are thus completely known". This application was refined by a variety of scientists over the 20th century including the Hartree-Fock approximation, the utilization of an iterative algorithm developed by Roothaan and Hall, and the use of basis sets formed from Gaussian functions.

1.2 Schrödinger Equation and the wave function

Towards the start of the 20th century, physicists came to the intriguing conclusion that position and momentum of atomic-sized particles could not be simultaneously measured, in direct contrast with conventional understanding. This was initially attributed to deficiencies in the experimental design although it was later postulated that this was a fundamental feature independent of how the measurement occurred. Indeed additional quantities were found to exhibit this incompatibility such as the z-component of angular momentum and the other two components of angular momentum for a particle. Pairs of observables such as these became known as incompatible observables. The extent of the certainty one can have of incompatible observables is described by the Heisenberg uncertainty principle, Eq. (1) shows this for position and momentum. This was a principle which is distinctly quantum and goes against a fundamental feature of classical mechanics which is the ability for a particle to have both a definite momentum (and hence velocity) and a definite position simultaneously.

$$\Delta x \Delta p \leq \frac{\hbar}{2} \tag{1}$$

where Δx is the uncertainty in one-dimensional position, Δp is uncertainty in one-dimensional momentum and $\hbar$ is Planck's constant divided by 2π.

Newton's laws rely upon a knowledge of the position and velocity of an object simultaneously at any time. From these, along with details of the forces on the object, it is possible to predict the future trajectory. The application of Newton's laws could not be applied to quantum particles because it was found that quantum particles cannot have simultaneous values for position and velocity. Aside from the inability to use Newton's laws to explain

time evolution, a perhaps more fundamental problem in the development of quantum mechanics was to develop a suitable description of the state of a particle. In classical mechanics the state of a particle could be fully described by the values of two variables, position and momentum. In quantum mechanics it was found that the use of a wavefunction was required, a complex-valued function of the translational degrees of freedom of the particle, usually chosen to be the three Cartesian coordinates. The classical mechanical particle description requires a two-dimensional vector, whereas the quantum mechanical wavefunction can in general only be described by an infinite-dimensional vector. The vector spaces where wavefunctions lie are known as Hilbert spaces and are a particular type of infinite-dimensional complex inner-product vector space.

The time-dependent Schrödinger equation is the solution to the problem of time-evolution of quantum particles, the quantum mechanical analogue of the classical Newton's second law. If the wavefunction of a particle is known at a specific time, the time-dependent Schrödinger equation can return the wavefunction of the particle for all later times. For additional detail consult Ref [6].

The theory of quantum mechanics attributes a mathematical operator to every physical observable. Particularly important operators include the Hamiltonian, which is the operator for energy, and the position and momentum operators. These operators are Hermitian and have an infinite number of eigenstates, which belong in the same vector space as wavefunctions of the particle in question. Indeed the particle has the potential to be described by any one of these eigenstates as its wavefunction. If the particle was to be described by a particular eigenstate then the observable corresponding to that operator would have a definite value. This definite value would be the eigenvalue corresponding to that eigenstate. This is a fundamental postulate of quantum mechanics. The quantum concept of discrete energy levels is described by this postulate. A quantum system can only ever have values for energy which are also eigenvalues for the Hamiltonian of that system. The problem of finding the eigenvalues and eigenstates of an operator is known as the eigenvalue problem for that operator.

In cases where the system is not described by an eigenstate for the observable we are interested in, experimental measurement could result in any one of a number of possible values, which occur with different probabilities. However, it is possible to produce a quantum average, known as an expectation value, which is the probability-weighted average of these possible values. For a system which has a definite value for a certain observable, the expectation value would be equal to this definite value. For other states the expectation value would in general not be equal to a possible value for this observable and therefore is

not a value which can actually be attained through a single measurement of the individual quantum system.

1.3 The application of quantum mechanical methods to chemistry

Quantum chemistry is the field concerned with the quantum mechanical description of electrons in atoms and molecules. It predominantly involves finding the eigenvalues and eigenstates of the Hamiltonian, based upon the observation that molecules tend to belong to these eigenstates and that quantities of interest can be derived from them. Although beyond the scope of this discussion, these eigenvalues and eigenstates can also be used to describe the time evolution of any wavefunction the system can be described by. For an atom or molecule the eigenstates of the Hamiltonian are none other than the electronic states familiar to chemists.

A complete solution to the Hamiltonian eigenvalue problem would produce the wavefunctions for all possible electronic states. It is well known to chemists that the energy gap from ground state to excited states is usually large for atoms and molecules, therefore often the ground state alone gives an adequate representation of the system. For this reason it is common to focus efforts on the eigenvalue problem for the lowest energy eigenstate, investigating higher electronic states only when they are required. A convenient method to do this uses the variational principle, described later.

Before attempts can be made to solve the eigenvalue problem for the Hamiltonian, otherwise known as the time-independent Schrödinger equation, it is first necessary to formulate a suitable Hamiltonian to describe the system, be it an atom or a molecule.

The general form of a Hamiltonian in one dimension is

$$(-\frac{\hbar^2}{2m}\frac{d^2}{dx^2} + V(x))\psi(x) = E\psi(x) \tag{2}$$

where m is the mass of the particle and $V(x)$ is the potential the particle is subject to.

Extending the problem to three-dimensions and replacing the potential with that derived from Coulomb's law for a single electron in the field of a single proton, fixed at the origin, we obtain

$$(-\frac{\hbar^2}{2m}\nabla^2 - \frac{e^2}{4\pi\epsilon_0 r})\psi(x,y,z) = E\psi(x,y,z) \tag{3}$$

where ∇ is the three-dimensional Laplacian differential operator, $\nabla^2 = \frac{\partial^2}{\partial x^2} + \frac{\partial^2}{\partial y^2} + \frac{\partial^2}{\partial z^2}$, e is the charge of an electron, ϵ_0 is the vacuum permittivity constant, r is the distance between electron and nucleus.

This is the Hamiltonian of the hydrogen atom problem which can be solved exactly and produces the familiar 1s, 2s, 2p, ... orbitals which dominate chemical understanding of structure and reactions. These familiar orbitals are solutions to a particularly simple one-electron Hamiltonian and their use to describe chemical species other than one-electron atoms is only ever approximate. To solve for the electronic structure of systems with greater than one electron it is necessary to develop a Hamiltonian which includes a far greater number of terms.

1.4 Born Oppenheimer approximation

The vast difference in mass between electrons and nuclei results in the positions of nuclei being largely independent of the instantaneous movement of electrons. The Born-Oppenheimer approximation simplifies the full Hamiltonian such that nuclei are treated as fixed point charges as opposed to quantum particles whose coordinates would be needed to be included into the wavefunction. The Hamiltonian and the wavefunction solutions are therefore dependent only on electronic coordinates as variables, with the nuclear positions being parameters only.

Solutions produced with this approximation are in very good agreement with those produced with the use of a more accurate Hamiltonian. Only in very high accuracy work is this approximation generally relinquished, indeed it is likely that relativistic effects would also need to be included in such work.

$$(-\hbar^2 \sum_{i=1}^{N} \frac{\nabla_i^2}{2m_i} + \sum_{i<j} \frac{e^2}{4\pi\epsilon_0 r_{ij}} - \sum_{i=1}^{N} \sum_{A=1}^{M} \frac{Z_A e^2}{4\pi\epsilon_0 R_{Ai}})\psi(r_1, \ldots, r_N) = E\psi(r_1, \ldots, r_N) \qquad (4)$$

where r_{ij} is the distance between electron i and electron j, Z_A is the integer charge of nucleus A and R_{Ai} is the distance from nucleus A to electron i. r_i represents (x_i, y_i, z_i), a vector containing the spatial coordinates of electron i. This is a convenient notation which can be used for many-electron wavefunctions and is frequently used in literature.

1.5 Variational principle

Despite the Born-Oppenheimer simplification the Schrödinger equation requires additional techniques to allow it to be solved. A particularly useful method, called the variational method, replaces an eigenvalue problem with that of optimization of a functional. A functional being a function whose value depends on one or more functions as opposed to variables. It can readily be implemented to approximate the lowest energy eigenfunction although can also be used to approximate other energy eigenfunctions with slight modifications. [6]

Theorem. The functional $F = \frac{\langle\psi|H|\psi\rangle}{\langle\psi|\psi\rangle}$ for $|\psi\rangle \in \mathcal{H}$ has lower bound E_0. Furthermore the wavefunctions $|\psi\rangle$ such that $H|\psi\rangle = E_0|\psi\rangle$ are exactly those which minimize the functional to its lower bound. $\mathcal{H}$ is the Hilbert space for the system, a complex inner-product vector space.

Proof. It is first noted that the functional is invariant to scaling by $c \in \mathbb{C}$. Let

$$|\psi'\rangle = c|\psi\rangle \tag{5}$$

so that by taking the adjoint of the equation

$$\langle\psi'| = c^*\langle\psi| \tag{6}$$

hence

$$\frac{\langle\psi'|H|\psi'\rangle}{\langle\psi'|\psi'\rangle} = \frac{|c|^2\langle\psi|H|\psi\rangle}{|c|^2\langle\psi|\psi\rangle} = \frac{\langle\psi|H|\psi\rangle}{\langle\psi|\psi\rangle} \tag{7}$$

Thus the value of the functional is invariant to scaling of the wavefunction. Without loss of generality it is then possible to restrict the domain to the subset of normalized wavefunctions, $\{|\psi\rangle \in \mathcal{H}$ such that $\langle\psi|\psi\rangle = 1\}$.

Since H is a Hermitian operator, $H^\dagger = H$, and according to the spectral theorem there exists an orthonormal basis of the Hilbert space consisting of eigenfunctions of that operator. We use this theorem and show that any state $|\psi\rangle \in \mathcal{H}$ can be expanded in terms of energy eigenfunctions. Let E_i be the eigenvalue corresponding to basis state $|\psi_i\rangle$ then

$$|\psi\rangle = \sum_{i=0}^{\inf} c_i|\psi_i\rangle \tag{8}$$

where c_i is the expansion coefficient for $|\psi_i\rangle$.

$$\frac{\langle\psi|H|\psi\rangle}{\langle\psi|\psi\rangle} = \langle\psi|H|\psi\rangle \text{ due to normalization} \tag{9}$$

$$\begin{aligned}
\langle\psi|H|\psi\rangle &= \sum_{i=0}^{\inf}\sum_{j=0}^{\inf} c_i^* c_j \langle\psi_i|H|\psi_j\rangle \\
&= \sum_{i=0}^{\inf}\sum_{j=0}^{\inf} c_i^* c_j E_j \langle\psi_i|\psi_j\rangle \\
&= \sum_{j=0}^{\inf} c_j^* c_j E_j \text{ due to the orthogonality of basis states} \\
&\geq \sum_{j=0}^{\inf} c_j^* c_j E_0 \\
&= E_0 \sum_{j=0}^{\inf} c_j^* c_j \\
&= E_0 \text{ by normalization of } |\psi\rangle \text{ and use of Eq. (8)}
\end{aligned} \tag{10}$$

For the second part of the theorem it is first noted that if $|\psi\rangle$ is such that $H|\psi\rangle = E_0|\psi\rangle$ then

$$\langle\psi|H|\psi\rangle = E_0\langle\psi|\psi\rangle = E_0 \tag{11}$$

Conversely if $E_0 = \langle\psi|H|\psi\rangle$ then Eq. (10) is an equality implying that $c_j = 0$ for all $j \neq 0$ and $c_0 = 1$ therefore by Eq. (8), $|\psi\rangle = |\psi_0\rangle$ hence $H|\psi\rangle = E_0|\psi\rangle$. This completes the proof of the latter statement of the theorem.

□

The importance of the first statement of the theorem is that if the functional F is minimized, the value it is minimized to will be the exact energy of the ground state. Furthermore the latter statement of the theorem ensures that whenever the functional is globally minimized (minimized over the entire Hilbert space), the wavefunction which allows this minimization will be the ground state wavefunction.

In practice this theorem is applied in an approximate way. It is not possible to minimize over the entire Hilbert space and therefore a subspace of this is used. In which case an assumption is made whereby the minimum functional value within this subspace is an approximation to E_0 and the corresponding wavefunction is an approximation to the exact ground state. It is found that E_0 can often be approximated well by a carefully chosen subspace involving antisymmetrized products of orbitals expanded in terms of atomic orbital-type functions, described in a later section on basis sets.

1.6 Many-particle wavefunctions

One-dimensional problems describe a single particle free to move in only one dimension, for example the particle in a one-dimensional box. Problems of this sort admit wavefunction solutions which are functions of one variable. Due to the simplicity of such problems they can often be solved exactly, as is the case for the particle in a box. When the system is extended to allow the particle movement within three-dimensional space, the wavefunction then becomes a function of three spatial variables.

When attempting to formulate and solve systems containing a number of particles, particle interaction generally prohibits the possibility to solve the system by use of separate wavefunctions for each particle. Many-particle wavefunctions must therefore be produced. Omitting spin, each particle would require three spatial variables to describe the wavefunction. Thus a wavefunction containing two particles in three-dimensional space would be a function of six variables, $(x_1, y_1, z_1, x_2, y_2, z_2)$, the former three concerning particle one, the latter three, particle two. It is clear that for systems such as moderately sized molecules the

Hamiltonian and wavefunction solutions could be dependent on hundreds of variables. These discussions hold strictly for particles of zero spin unlike electrons. The number of variables the wavefunctions depends upon is increased by one per particle by including spin.

1.7 Indistinguishability of particles

Consider the Born interpretation of a wavefunction in one dimension: $\rho(x) = |\psi(x)|^2$ where $\rho(x)$ is the probability density function, prenormalized to 1 over the real line assuming $\psi(x)$ is normalized. This equation gives the relative probability of finding the electron at position x. The Born interpretation can be extended to many particles in three-dimensions in which case we form a probability density function such as $\rho(x_1, y_1, z_1, x_2, y_2, z_2)$ for two particles. This gives us the relative probability of finding particle one at (x_1, y_1, z_1) and particle two simultaneously at (x_2, y_2, z_2), but only if the particles are distinguishable. If the particles are indistinguishable for example electrons within a molecule, the probability is only formal since it is impossible to say tell which particle is particle one and which is particle two. Therefore it is impossible to state conclusively that particle one is at (x_1, y_1, z_1) and particle two is at (x_2, y_2, z_2), whereas it is possible to state that there are two particles, one of which is at (x_1, y_1, z_1), the other at (x_2, y_2, z_2).

For a correct wavefunction to be obtained it is imperative that indistinguishability of electrons is respected, therefore the following formal probabilities must be equal.

$$\rho(x_1, y_1, z_1, x_2, y_2, z_2) = \rho(x_2, y_2, z_2, x_1, y_1, z_1) \tag{12}$$

Therefore implying

$$|\psi(x_1, y_1, z_1, x_2, y_2, z_2)|^2 = |\psi(x_2, y_2, z_2, x_1, y_1, z_1)|^2 \tag{13}$$

$$\Longleftrightarrow$$

$$\psi(x_1, y_1, z_1, x_2, y_2, z_2) = e^{i\theta}\psi(x_2, y_2, z_2, x_1, y_1, z_1) \tag{14}$$

where θ is any real number.

There is no mathematical reason which states which theta is to be used. Indeed complicated senarios could be imagined in which particles change theta with time or when placed in fields, without contradicting any other principle of quantum mechanics. All experiments so far have concluded that only values of theta corresponding to sign retention and sign inversion are observed and that particles of a certain type only ever exhibit one or other of these two behaviours. Particles obeying retention of wavefunction upon a single transposition of particles are known as bosons, particles for which the wavefunction undergoes a sign inversion

upon transpositions are known as fermions and this class includes the electron. For this reason wavefunction solutions to the Schrödinger equation must include sign inversion upon particle transposition, a feature known as antisymmetry, if they are to represent a system of electrons. A determinant is a convenient structure for forming antisymmetric wavefunctions and will be investigated further in the chapter on Slater determinants.

1.8 Spin

Discovered by the Stern-Gerlach experiment, spin is a purely quantum mechanical phenomenon which electrons and many other subatomic particles possess. It is an angular momentum not accounted for by orbital angular momentum which is the classical analogue of angular momentum caused by circular motion around a nucleus. The mechanics of spin are presented in Ref [6]. In order to form a valid wavefunction describing the system of particles, the spin of each electron must be included. For each electron there exist two possible spin states, described mathematically by two spin functions $\alpha(\omega)$, and $\beta(\omega)$ where ω is the so-called spin variable. These obey the following normalization and orthogonality constraints.

$$\int \alpha(\omega)^* \alpha(\omega) d\omega = 1 \tag{15}$$

$$\int \alpha(\omega)^* \beta(\omega) d\omega = 0 \tag{16}$$

$$\int \beta(\omega)^* \beta(\omega) d\omega = 1 \tag{17}$$

Each particle will therefore contribute four variables to the wavefunction; three spatial and one spin.

Earlier it was shown that the three spatial variables could be recorded as a single variable labelled r_i for electron i. Similarly for a set of four variables the symbol x_i is used. x_i therefore represents $(x_i, y_i, z_i, \omega_i)$ and (r_i, ω_i).

1.9 Slater determinants

Two related properties which many-electron wavefunctions must have are the indistinguishability of particles and the closely related antisymmetry principle. Both are conveniently satisfied by determinants, known in this context as Slater determinants. Unlike their use in elementary matrix algebra, these are now applied to functions rather than to numbers.

$$\psi(x_1, \ldots, x_N) = \frac{1}{\sqrt{N!}} \begin{vmatrix} \chi_1(x_1) & \ldots & \chi_N(x_1) \\ \vdots & \ddots & \vdots \\ \chi_1(x_N) & \ldots & \chi_N(x_N) \end{vmatrix} \tag{18}$$

where $\chi(x_i)$ is a single-electron function known as a spin orbital, for electron i.

A transposition of electron coordinates is equivalent to a transposition of rows, leading to the regeneration of the determinant but with a negative sign. This is demonstrated by a three electron Slater determinant but extends to N-electron Slater determinants and shows that these wavefunctions satisfy the antisymmetry principle.

$$\frac{1}{\sqrt{6}}\begin{vmatrix}\chi_1(x_1) & \chi_2(x_1) & \chi_3(x_1)\\ \chi_1(x_2) & \chi_2(x_2) & \chi_3(x_2)\\ \chi_1(x_3) & \chi_2(x_3) & \chi_3(x_3)\end{vmatrix} = -\frac{1}{\sqrt{6}}\begin{vmatrix}\chi_1(x_1) & \chi_2(x_1) & \chi_3(x_1)\\ \chi_1(x_3) & \chi_2(x_3) & \chi_3(x_3)\\ \chi_1(x_2) & \chi_2(x_2) & \chi_3(x_2)\end{vmatrix}$$

The formula for an N-electron Slater determinant is shown in Eq. (19).

$$\psi(x_1,\ldots,x_N) = \frac{1}{\sqrt{N!}}\sum_{\sigma\in S_N} sgn(\sigma)[\chi_1(x_{\sigma(1)})\ldots\chi_N(x_{\sigma(N)})] \tag{19}$$

where S_N is the symmetric group of order N containing $N!$ permutations denoted σ, and $sgn(\sigma)$ is the signature of the permutation.

It can be seen that the determinant is a sum of $N!$ products of single-electron functions. Indistinguishability of particles can be seen from how each single-electron function is occupied by each electron equally through the summation.

The use of Slater determinants reduces the problem of forming an N-electron wavefunction into one of forming appropriate single-electron functions, with no further concern over indistinguishability nor antisymmetry. It is common to interpret these spin orbitals as each containing an electron and this has led to the successful field of molecular orbital theory. However this is a simplification because higher level calculations require additional modifications on the wavefunction. One such modification involves the inclusion of additional determinants into a single sum, however the simple interpretation of a single-electron function per electron must be replaced by the concept of fractional orbital occupations.

Usually we seek spin orbitals to be both normalized and orthogonal with respect to the typical single-particle function space inner product

$$\int \chi_i(x)^*\chi_j(x)dx = \delta_{ij} \tag{20}$$

where δ_{ij} is the Kronecker delta defined as

$\delta_{ij} = 1$ if $i = j$

$\delta_{ij} = 0$ if $i \neq j$.

Orthogonality of spin orbitals is not essential, but is usually imposed to make matrix elements between determinants simpler and to retain the simple normalization constant $\frac{1}{\sqrt{N!}}$

multiplying the determinant. Expressions for matrix elements between determinants which are not necessarily orthogonal are presented in Ref [7].

In forming Slater determinant wavefunctions it is usually assumed we have a set of K spin orbitals, N of which are occupied $\chi_1, \chi_2, \ldots, \chi_N$ and $K - N$ of which are unoccupied $\chi_{N+1}, \chi_{N+2}, \ldots, \chi_K$. Often the indicies of the occupied orbitals are denoted by the letters $a, b, c, \ldots$ and unoccupied by the letters $r, s, t, \ldots$.

Spatial orbitals are single-particle functions of three spatial coordinates only, therefore are functions of r_i as opposed to x_i. A spatial orbital can be made into a spin orbital by multiplication of a spin function, of which there are only two possibilities for single electrons.
$\chi(x) = \psi(r)\alpha(\omega)$
$\chi(x) = \psi(r)\beta(\omega)$

Most ground state wavefunctions for stable molecules are spin singlets and are represented by the totally symmetric irreducible representation. Such wavefunctions are most readily formed by a restricted closed shell assumption. The term *restricted* implies that wavefunctions are built up through pairs of spin orbitals, each with the same spatial orbital but with different spin functions. The molecular orbital interpretation states that each molecular orbital (corresponding to spatial orbitals) can contain two electrons of differing spin. The restricted assumption is largely accurate for most closed shell species. The chemical intuition of electrons appearing as pairs is largely reproduced in the accuracy of the restricted assumption. An *unrestricted* wavefunction is also built up using pairs of spin orbitals, however the spatial functions corresponding to each spin within a spin orbitals pair are permitted to differ to a small degree. The term *closed shell* means that no spin orbital appears without a spin-paired counterpart, therefore no electrons are left unpaired.

1.10 Matrix elements of determinants

The exact ground state wavefunction has energy E_0, however by the variational theorem all approximate wavefunctions will have a higher energy. It is not possible to find the ground state wavefunction exactly so approximations must be made. The use of single-determinantal theory, wavefunctions composed of just one Slater determinant, is one such approximation. Approximate wavefunctions are not eigenfunctions of the Hamiltonian, therefore such states cannot strictly be said to have an unique well-defined energy. The problem is bypassed by using the quantum average of the energy of a state, otherwise called the energy expectation value, $\langle\psi|H|\psi\rangle$. From this point on, the distinction between energy and energy expectation value is relaxed, referring to the latter by the term energy.

The problem of approximating the ground state wavefunction becomes one of varying parameters in the trial wavefunction in order to minimize the energy. If this minimizing value is close to E_0 it can be assumed that the corresponding wavefunction will be similar to the exact ground state. Calculating the energy of a Slater determinant is one of a more general set of problems of finding matrix elements between these determinants. The results are known as the Slater-Condon rules and are presented below without proof (adapted from Ref [8]).

$|\psi\rangle$ represents a normalized Slater determinant.

$|\psi_a^r\rangle$ represents a normalized Slater determinant which differs from the reference Slater determinant, $|\psi\rangle$, by replacement of spin orbital χ_a of the occupied set with χ_r of the unoccupied set.

$|\psi_{ab}^{rs}\rangle$ represents a normalized Slater determinant which differs from the reference Slater determinant, $|\psi\rangle$, by replacement of spin orbitals χ_a and χ_b of the occupied set with χ_r and χ_s of the unoccupied set.

$\langle\psi|\psi_a^r\rangle = 0$ assuming $a \neq r$

$|r\rangle$ is the Dirac notation representation of $\chi_r(x_1)$

$|rs\rangle$ is the Dirac notation representation of $\chi_r(x_1)\chi_s(x_2)$

$h(i) = -\frac{\hbar^2}{2m_i}\nabla_i^2 - \sum_{A=1}^{M} \frac{Z_A e^2}{4\pi\epsilon_0 R_{Ai}}$

$g(i,j) = \frac{e^2}{4\pi\epsilon_0 r_{ij}}$

Assuming the one-electron operator is of the form $O_1 = \sum_{i=1}^{N} h(i)$ we have that

$\langle\psi|O_1|\psi\rangle = \sum_{i=1}^{N} \langle i|h|i\rangle$

$\langle\psi|O_1|\psi_a^r\rangle = \langle a|h|r\rangle$

$\langle\psi|O_1|\psi_{ab}^{rs}\rangle = 0$

Assuming the two-electron operator is of the form $O_2 = \sum_{i=1}^{N}\sum_{j=i+1}^{N} g(i,j)$ we have that

$\langle\psi|O_2|\psi\rangle = \sum_{i=1}^{N}\sum_{j=i+1}^{N} (\langle ij|g|ij\rangle - \langle ij|g|ji\rangle)$

$\langle\psi|O_2|\psi_a^r\rangle = \sum_{i=1}^{N} (\langle ai|g|ri\rangle - \langle ai|g|ir\rangle)$

$\langle\psi|O_2|\psi_{ab}^{rs}\rangle = \langle ab|g|rs\rangle - \langle ab|g|sr\rangle$

The Hamiltonian is a sum of one and two electron operators.

$$H = \sum_{i=1}^{N} h(i) + \sum_{i=1}^{N} \sum_{j=i+1}^{N} g(i,j) \tag{21}$$

This leads to a formula, Eq.(23), for E, the expectation value of the Hamiltonian for the Slater determinant wavefunction.

$$E = \langle\psi|H|\psi\rangle = \langle\psi| \sum_{i=1}^{N} h(i) + \sum_{i=1}^{N} \sum_{j=i+1}^{N} g(i,j)|\psi\rangle \tag{22}$$

$$= \sum_{i=1}^{N} \langle i|h|i\rangle + \sum_{i=1}^{N} \sum_{j=i+1}^{N} (\langle ij|g|ij\rangle - \langle ij|g|ji\rangle) \tag{23}$$

When the many-electron wavefunction is formulated as a Slater determinant consisting of spin functions the matrix elements between many-electron wavefunctions are reduced to matrix elements of one and two-electron operators.

1.11 Hartree-Fock approach

In the previous sections, the problem of forming a suitable many-electron wavefunction was reduced to one of finding a set of single-electron functions known as the spin orbitals. We now proceed to discuss how a suitable set of spin orbitals can be generated thus enabling an approximate solution to be obtained.

The Hartree-Fock approach is a method to produce spin orbitals so that the energy of a single Slater determinant is minimized. These spin orbitals are generated as eigenfunctions of a single-electron operator known as the Fock operator. This operator is artificial insofar as it does not represent any physical observable. The derivation of the Hartree-Fock equation involves the use of the mathematical theory of functional analysis and is not presented here. However the Fock operator is constructed so that its lowest N eigenfunctions can be used in a single Slater determinant wavefunction which minimizes the energy. In the limit of an exact solution to the Fock operator eigenvalue problem, the Slater determinant produced is said to achieve the Hartree-Fock limit and represents the lowest energy which a single Slater determinantal wavefunction can achieve. The Hartree-Fock equation is presented in Eq. (24).

$$f(x_1)\chi_a(x_1) = \epsilon_a\chi_a(x_1) \tag{24}$$

where $f(x)$ is the Fock operator and χ_a, an eigenfunction, is a spin orbital.

A significant problem with any single-determinantal wavefunction is the lack of full consideration of electron correlation. *Electron correlation* is the phenomenon where the position

and motion of each electron is affected by the position and motion of the other electrons in the system. In particular although electrons of parallel spin are correlated, in so called exchange correlation, there is a lack of correlation between antiparallel spins. This defect is often minimal for qualitative descriptions of simple electronic states, but for moderate and higher level work further correlation effects must be included beyond a Hartree-Fock wavefunction. These methods frequently use multiple determinants, for example configurational interaction (CI) and complete active-space self-consistent field (CASSCF), both discussed later.

1.12 Basis sets

The Hartree-Fock equation cannot be solved directly and is most commonly solved approximately using a basis set. In quantum chemistry a basis set is a finite set of three-dimensional spatial functions usually representing atomic orbitals. The span of a basis set consisting of K-functions is a K-dimensional vector space within which the Hartree-Fock equations can be solved using techniques of linear algebra. The solutions will be linear combinations of the K basis functions, each of which being an approximation to successive eigenfunctions of the Fock operator. A greater number of basis functions means that the equation is solved over a larger vector space and the solutions can better approximate the exact Fock operator eigenfunctions. A wiser choice of basis functions means that a better approximation to these exact eigenfunctions can be produced from a smaller vector space.

It is found that the solutions to the Hartree-Fock equation closely resemble linear combinations of atomic orbitals and for this reason the basis set chosen usually involves a series of functions which closely resemble atomic orbitals. Atomic orbitals themselves behave as e^{-ar} as $r \to \infty$, belonging to a class called Slater-type orbitals (STOs), Eq. (25) is an example of a 1s STO. When solving for matrix elements between Slater determinants, STOs produce two-electron integrals which are very difficult to solve. These orbitals are usually approximated by short linear combinations of so-called Gaussian-type orbitals (GTOs) involving different values of α, known as the orbital exponent. Gaussian-type orbitals have one and two-electron integrals which can be solved analytically rather than necessarily through numerical techniques, therefore these integrals are considerably less computationally expensive to calculate.

$$\phi_{1s}^{STO}(\zeta, r - R_A) = (\frac{\zeta^3}{\pi})^{\frac{1}{2}} \exp(-\zeta|r - R_A|) \tag{25}$$

where ζ is the Slater orbital exponent.

$$\phi_{1s}^{GTO}(\alpha, r - R_A) = (\frac{2\alpha}{\pi})^{\frac{3}{4}} \exp(-\alpha|r - R_A|^2) \tag{26}$$

where α is the Gaussian orbital exponent.

There are many possible choices of basis sets but a common choice are known as Pople basis sets. As an illustration the basis set denoted 6-31G* is described. Pople basis sets are characterized by the capital letter G in the name of this basis set. This indicates that the basis set involves linear combinations of Gaussian functions to approximate Slater-type orbitals, rather than using the STOs directly. The hyphen indicates this is a split-valence basis set, meaning that inner shell orbitals are represented by single basis functions, whereas valence orbitals are represented by two or more slightly different basis functions. This reflects the fact that inner shell orbitals change very little upon bonding, whereas valence orbitals can change significantly, therefore the calculation permits greater variational flexibility to the valence orbitals by including more of them into the basis set. The initial number in the 6-31G* basis set indicates that the inner shell orbitals are each represented by one basis function which is a linear combination of six Gaussian functions. The two numbers after the hyphen indicate that each valence orbital is represented by two basis functions (a so-called double zeta basis set), one of which is a linear combination of three Gaussian functions, the other a single Gaussian function. Finally the asterisk after the letter G indicates the inclusion of polarization functions, additional basis functions representing the next set of unoccupied d-type orbitals on atoms beyond hydrogen. If a further asterisk is added, 6-31G**, additional basis functions would be requested which represent p-type orbitals on hydrogen.

1.13 Self-consistent field procedure

The finite-dimensional vector space over which the equation will be solved is defined once a basis set has been specified. The Hartree-Fock equation can then be solved using techniques of linear algebra. A series of matrices must be defined before the matrix form of the Hartree-Fock equation can be stated. This presentation closely follows Ref [8].

C is the coefficient matrix, a square matrix where each column represents the components of the basis functions for each orbital. When the equation has been solved, C will have columns being the eigenvectors of the Fock matrix. These will correspond to the linear combinations of basis functions which make up the orbitals required for the Slater determinant.

$F(C)$ is the Fock matrix which depends on the coefficient matrix C. The matrix is defined through its matrix elements.

$$F_{\mu\lambda} = \langle \phi_\mu | f | \phi_\lambda \rangle$$

where f is the Fock operator adapted to act on spatial, as opposed to spin orbitals.

S is known as the overlap matrix and reflects the fact that the basis functions are not generally orthogonal. This is most immediately clear by noting that we have basis functions

positioned, in general, on different nuclei around the molecules hence these functions are expected to have non-zero overlap integrals which vary dependent on nuclear positions. The matrix is defined through its matrix elements.

$$S_{\mu\lambda} = \langle \phi_\mu | \phi_\lambda \rangle$$

ϵ is a diagonal matrix containing the eigenvalues of matrix F for each of the eigenvectors within the coefficient matrix C.

The Hartree-Fock equation

$$f(x_1)\chi_a(x_1) = \epsilon_a \chi_a(x_1) \tag{24}$$

can be transformed to act solely within a finite-dimensional vector space

$$F(C)C = SC\epsilon \tag{27}$$

representing a set of linear equations known as the Roothaan equations. This is a generalized eigenvalue problem for the Fock and overlap matrices. The term 'generalized' is used because of the inclusion of the overlap matrix S.

The dependance of the Fock matrix on the coefficient matrix results in these equations having to be solved iteratively. The correct Fock matrix requires knowledge of the final coefficient matrix in order to define it, however until the problem has been solved it is not possible to know this matrix. In practice a guess at the coefficient matrix is obtained in order to form an approximate Fock matrix for which we can obtain a new, usually far better, approximation to the coefficient matrix via solving the Roothaan equations. The procedure is repeated until the Roothaan equations achieve self-consistency; the coefficient matrix used in the formation of the Fock matrix differs negligibly from the coefficient matrix obtained via the generalized eigenvalue problem for this Fock matrix.

1.14 Configurational interaction

As described earlier a significant drawback to the Hartree-Fock approach is the lack of correlation between electrons with antiparallel spins, the inclusion of which can generally produce wavefunctions of far greater accuracy. Methods which improve upon the Hartree-Fock approach are known as post-Hartree-Fock methods. Configurational interaction (CI) is one of the most conceptually simple post-Hartree-Fock methods.

Configurational interaction is a many-determinantal theory which is applied once an initial Hartree-Fock wavefunction has been formed. The resulting wavefunction is a linear combination of so-called configurations, single determinants or short linear combinations of determinants known as spin-adapted configurations which have well-defined spin states. The configurations themselves can be used in linear combinations and the coefficients optimized in order to minimize the energy. In other words once a set of configurations are defined, their span produces a finite-dimensional vector space over which we can optimize the energy. The greater the number of configurations, the greater the dimension of this vector space and the more variational flexibility is available for energy minimization.

Configurations are formed through so-called substituted determinants. A k-tuply substituted determinant involves a replacement of k occupied spin orbitals in the ground state Hartree-Fock wavefunction with k unoccupied spin orbitals.

The notations for singly and doubly substituted determinants are presented below, based on a reference Slater determinant $|\psi\rangle$.

$$|\psi\rangle = \frac{1}{\sqrt{N!}} \begin{vmatrix} \chi_1(x_1) & \dots & \chi_a(x_1) & \chi_b(x_1) & \dots & \chi_N(x_1) \\ \dots & \dots & \dots & \dots & \dots & \dots \\ \chi_1(x_N) & \dots & \chi_a(x_N) & \chi_b(x_N) & \dots & \chi_N(x_N) \end{vmatrix} \tag{28}$$

$$|\psi_a^r\rangle = \frac{1}{\sqrt{N!}} \begin{vmatrix} \chi_1(x_1) & \dots & \chi_r(x_1) & \chi_b(x_1) & \dots & \chi_N(x_1) \\ \dots & \dots & \dots & \dots & \dots & \dots \\ \chi_1(x_N) & \dots & \chi_r(x_N) & \chi_b(x_N) & \dots & \chi_N(x_N) \end{vmatrix} \tag{29}$$

$$|\psi_{ab}^{rs}\rangle = \frac{1}{\sqrt{N!}} \begin{vmatrix} \chi_1(x_1) & \dots & \chi_r(x_1) & \chi_s(x_1) & \dots & \chi_N(x_1) \\ \dots & \dots & \dots & \dots & \dots & \dots \\ \chi_1(x_N) & \dots & \chi_r(x_N) & \chi_s(x_N) & \dots & \chi_N(x_N) \end{vmatrix} \tag{30}$$

A significant drawback to the use of configurational interaction in practical applications is the lack of size consistency. Size consistency is a situation where, assuming the level of the CI method is fixed (to what degree the determinants are substituted), different accuracies are found for larger and smaller molecules. For example this manifests itself when the method is applied to two non-interacting molecules separated by a vast distance where an energy is produced which is not equal to the sum of those produced from each of the molecules separately, at the same level of CI. All practical uses of configurational interaction suffer severely from this problem.

1.15 CASSCF

Complete active-space self-consistent field (CASSCF) is a post-Hartree-Fock method frequently used to describe excited states as well as molecular complexes during bond formation and cleavage. To apply the method one must specify a number of orbitals and a number of electrons to be included in the active-space. These are typically the valence orbitals most important in the chemistry of the structure. The notation for this is frequently written as CASSCF[n,m] where n is the number of active-space electrons and m is the number of active-space orbitals. As an example benzene would typically be applied through a CASSCF[6,6] procedure where the six highest energy valence electrons would be placed within the three highest energy bonding orbitals and the three lowest energy antibonding orbitals. Within the active space the procedure considers all Slater determinants which can be formed from the n electrons in the m orbitals in any order. An energy optimization is then performed using either Slater determinants directly, or more commonly combining these into spin-adapted configurations in the same manner as in configurational interaction. The advantage of using spin-adapted configurations is that those of the incorrect spin can be discarded before performing the optimization, reducing computational cost.

The method belongs to a class known as multi-configurational self-consistent field (MCSCF) where both the orbital coefficients and the configuration coefficients are varied simultaneously. This is as opposed to both the Hartree-Fock method, where only the orbital coefficients are variational parameters, and configurational interaction where only the configuration coefficients are varied. Details are presented in Ref [8].

2 Isotropic magnetic shielding in the classification of aromaticities for low-lying electronic states of benzene and cyclobutadiene

2.1 Introduction and literature

2.1.1 The nature of aromaticity

The elusive concept of aromaticity is difficult to define, but is indicated by a wide range of properties often leading to dramatic structural reorganization and chemical behaviour in aromatic molecules in contrast to similar non-aromatic analogues. Despite having many indicators, no one in particular is an ideal measure of aromaticity, and similarly antiaromaticity. Reactivity criteria were the first used, indeed the unusual chemical behaviour of aromatic compounds led scientists to discover the concept of aromaticity in the first place. Michael Faraday was the first to characterize benzene, and noticed that despite the composition being one of an unsaturated hydrocarbon, its reactivity was very much unlike that typical for unsaturated hydrocarbons.

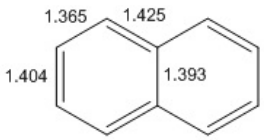

Figure 1: Experimental bond lengths in naphthalene. Bond lengths obtained from Ref [1].

Bond length equalization, and equivalently a heightening of symmetry, is a common feature observed in the formation of the large majority of aromatic compounds. This is most clearly seen when comparing benzene with 1,3,5-hexatriene. Unfortunately bond length equalization cannot be used as a criterion for determining aromaticity due to the presence of aromatic compounds which have very little bond equalization. This is significant in asymmetric aromatic systems such as substituted benzenes, which lose bond equalization with respect to benzene itself, without necessarily becoming any less aromatic. Another example is naphthalene which has large bond length variations but is still very much aromatic, see Figure 1.

The converse is also true because there exist non-aromatic molecules with bond equalization. Borazine, for example, has bond equalization despite the electrons being predominantly localized on the electronegative nitrogen atoms. Due to this weighting of the electron density on certain atoms, a significant π-ring current cannot be sustained and hence the molecule is only very weakly aromatic.[9]

For these reasons, energetic, rather than geometric, criteria are more commonly used to characterize aromaticity. Examples are aromatic stabilization energies (ASEs) and resonance energies (REs) which involve the calculation of the energy difference involved in hypothetical

reactions designed to isolate the energy involved in moving from individual isolated π-systems to ring π-systems. There are often many such hypothetical reactions available to calculate the energy of aromaticity, even for simple examples such as benzene in Figure 2.

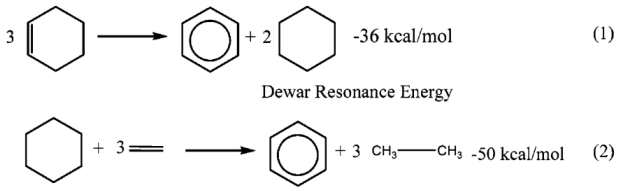

Figure 2: Hypothetical reactions to calculate the resonance energy for benzene. Image obtained from Ref [2].

As this simple example indicates, there can be a significant variation in the energies calculated due to the influence of other competing effects. Most significant are hyperconjugation and ring strain. Reaction scheme 1 has hyperconjugation between the double bond and adjacent C-H bonds which will artificially stabilize the reactants with respect to the products leading to a lower reaction energy value. Efforts can be made to standardize the types of reactions used to calculate ASEs and REs. The examples in Figure 2 are REs because they consider the complete energy of delocalization from separate double bonds. ASEs already start with conjugated systems, but consider the energy of forming a delocalized cycle out of these.

2.1.2 The use of NMR for characterization of aromaticity

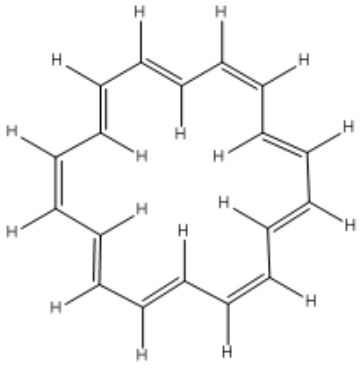

Figure 3: Structure of [18]annulene.

The use of NMR is the most popular experimental technique to determine the aromaticity of a system. Protons on benzene produce a ^{1}H NMR chemical shift of 7.3 ppm, in contrast to those bonded to the double bond of cyclohexene which have a shift of 5.6 ppm. Furthermore the opposite effect is seen within aromatic rings where a strong upfield shift is observed. Protons of [18]annulene for example resonate at 9.3 ppm outside the ring and -3.0 ppm within the ring. The 2.0 ppm increase for protons outside the ring compared to benzene can in-part be attributed to additional π-electrons. It is also interesting to note that the effects of aromaticity on protons inside the ring is far greater than that on those outside, as shown by the 3.7 ppm downfield displacement for outer protons as compared to cyclohexene contrasted with the 8.6 ppm upfield displacement for inner protons again compared to cyclohexene.

2.1.3 Nucleus independent chemical shift (NICS) and other magnetic techniques

NMR chemical shifts of various nuclei, both within and outside a ring system provide a common method to evaluate aromaticity, however it is intriguing to ask what could be deduced from magnetic shieldings at positions in space where the molecule does not hold NMR active nuclei. The magnetic shielding and the perturbation of the magnetic field which corresponds to it can be determined at any position in space around the molecule. The use of NMR being merely an experimental method of sampling the value of the isotropic shielding value at the positions of NMR active nuclei. The utility of NMR shifts for exploration of aromaticity provides sufficient justification to investigate how shielding might behave throughout the molecule, for instance at the centre of a delocalized ring.

Schleyer and coworkers introduced the use of nucleus independent chemical shifts (NICSs) in 1996 as a computational aromaticity probe.[3] These are defined as the negative of calculated absolute isotropic shielding values, $-\sigma_{iso}(r)$, where the isotropic shielding is defined as one-third the trace of the shielding tensor.

$$\sigma_{iso}(r) = \frac{1}{3}(\sigma_{xx} + \sigma_{yy} + \sigma_{zz}) \tag{31}$$

The NICS value tends to zero as the position where it is evaluated tends to infinite distance from the molecule. This means that all values can be given relative to zero and no reference molecule is required, nor any reaction schemes such as those needed for the evaluation of ASEs and REs.

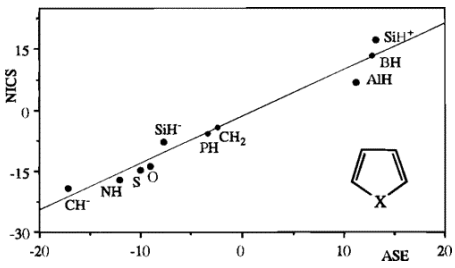

Figure 4: Correlation between NICs and ASEs for a variety of five-membered heterocycles. Image obtained from Ref [3].

Originally the NICS value for a given ring was determined at the non-weighted mean of positions of heavy atoms of the ring. With this definition, now frequently referred to as NICS(0), a strong positive correlation was determined against ASEs for a variety of five membered cycles with π-systems, see Figure 4.

Within a small number of years after the technique was introduced, it had found applications in the determination of aromaticity in a wide range of interesting molecules. These included rings containing mixtures of double and triple bonds[10], *closo*-boranes[11] and heteroaromatic bowl-shaped molecules[12].

The use of the NICSs technique is not limited to the NICS(0) index and it was found that other NICSs indices were better at describing relative aromaticity of molecules, as described in the following section.

Concerns have been frequently raised over the lack of experimental evidence supporting off-nuclear shieldings and whether any quantity derived solely through theory has any place in the discussion of molecular properties and characteristics. There are two possible counterarguments which can be used to justify the use of off-nuclear shieldings. One argument is that the isotropic shielding can be used to calculate the chemical shift at NMR active nuclei, hence for these particular positions the isotropic shielding can indeed be compared with experimental values. If the calculation produced these chemical shifts to high accuracy, this is strong justification, although by no means a proof, that the isotropic shielding at off-nuclear positions will be accurate too if there was a method to experimentally determine these. The other argument is that in some cases direct measurement of the isotropic shielding is possible.

Experiments have been devised which allow the determination of shielding at positions of interest other than on the positions of nuclei of the molecule. Although these have limited scope as routine methods for aromaticity characterization, they help to confirm the use of theoretical off-nuclear shieldings. A disadvantage of such a technique is that the inclusion of additional molecular species into the original molecule will perturb its wavefunction and hence will affect all derived quantities, including magnetic shieldings.

Li^+ ions frequently bind to the faces of delocalized ring systems. ^{7}Li NMR can then be used to determine the extent of the ring current and hence the aromaticity of the ring.[2] In most lithium-containing compounds, lithium is present as an ion, hence its NMR shift changes very little with different chemical situations. The exception is when bound to delocalized rings since the changes in shielding are now due to ring currents as opposed to purely via chemical bonding. Cyclopentadienyl lithium (LiCp) has a ^{7}Li shift of -8.60 ppm, whose upfield shift reflects the aromaticity of the cyclopentadienyl anion.[13]

Saunders and coworkers showed how atoms and small molecules could be experimentally inserted into fullerenes.[14] The NMR shifts could then be measured and compared with the relevant NICS values as a method to experimentally verify the NICSs technique. Bühl and Hirsch analysed NICS and NMR results for ^{3}He placed at the centre of various fullerenes and found good agreement.[15] Although Li^+ is a cation and therefore likely to strongly modify the electronic structure of the original molecule, a helium atom will also perturb the wavefunction of the original molecule, although to a lesser degree. This is because, despite being chemically inert it still introduces additional electrons into the system.

Before the NICS technique, magnetic susceptibility exaltations (χ) were frequently used to measure aromaticity. They are based on the difference in the magnetic susceptibility of the molecule and that of the sum of its atoms. In non-aromatic molecules it is usually quite accurate to sum contributions from each atom to find the value for the molecule as a whole. By considering the difference between the molecular magnetic susceptibility and the assembled magnetic susceptibility produces the magnetic susceptibility exaltation. Significant diatropic (negative) exaltations are an indication of aromaticity, likewise paratropic (positive) exaltations indicate antiaromaticity.

The magnetic susceptibility exaltation produces a value for the entire molecule unlike the NICS technique which produces values for every ring individually. It is useful to be able to analyse separate rings within a molecule. It also reflects the understanding that aromaticity is not a molecular property rather a property of rings within the molecule. A further noteworthy difference between the two techniques is that NICS values change only moderately with increases in ring size unlike exaltations which have an $area^2$ dependance.

2.1.4 Dissected NICSs and other NICSs indices

Schleyer and coworkers introduced the first NICS index,[3] later known as NICS(0), in 1996 but shortly after recommended the use of NICSs indices calculated at a position with some displacement perpendicular to the ring.[16] One such index which has become popular is the NICS(1) index, defined as $\sigma(r)_{iso}$ at 1 Å above the centre of the ring. The reason for this recommendation was because NICS(1) has a greater contribution from the π-ring current effects and less from local influences on the magnetic shielding.

Pursuing this idea further, Schleyer and coworkers investigated the use of dissected NICS in an attempt to decompose NICS values into π, σ and CH contributions using a localization procedure.[4] Localized molecular orbitals (LMOs) were produced from the canonical molecular orbitals using a localization procedure which permitted reliable $\pi - \sigma$ separation. The NICS value was then partitioned into contributions from all LMOs and the sum of contributions from all π-LMOs lead to a CC(π) value, those from C-C σ-LMOs led to a CC(σ) value and those from C-H σ LMOs lead to a CH value. To remove influence from local effects not important in aromaticity determination, the CC(π) values could be compared for various rings.

On going from NICS(0) to NICS(1) it was found that the CC(σ) and CH values reduced greatly whereas the CC(π) remained fairly large. This indicates that NICS(1) includes a greater proportion of CC(π) than NICS(0) hence supporting the recommendation of the use of NICS(1) if a detailed dissected NICS procedure is not within the scope of a given compu-

tational study. Despite the utility of NICS(1), the decision to evaluate NICS at precisely 1 Å above the ring is fairly arbitrary and better comparisons between differently sized rings could be achieved through modifying the distance used dependent on the ring area, for example. A more natural alternative presents itself with certain molecules, such as benzene, where the NICS value reaches a maximum in magnitude as the distance is traversed up the z-axis. Comparing these maximum values for different rings could be more successful than fixing a distance of 1 Å and doing all comparisons with respect to this.

A significant problem with the dissected NICS technique arises when it is applied to non-planar molecules. A vital feature of the localization procedure used is that it must successfully produce $\pi - \sigma$ separation and a popular choice is the Pipek-Mezey procedure.[17] Without $\pi - \sigma$ separation it is unclear whether an orbital contribution to the NICS value should contribute to CC(π), CC(σ) or CH. For this reason the commonly used Boys localization procedure[18] cannot be applied for dissected NICS. Unfortunately $\pi - \sigma$ separation of the Pipek-Mezey procedure can only reliably be produced when the ring is strictly planar.

NICS values are usually concerned with the isotropic shielding which is the trace of the shielding tensor. However since delocalized π-systems are comprised of p_z orbitals it is frequently considered that the zz-component of the shielding tensor is the component of greatest importance in aromaticity evaluation. This index is denoted $NICS_{zz}$ and is frequently calculated either at the ring centre or 1 Å above. In a study of correlations between a variety of NICS indices and ASEs of five-membered rings, $NICS(0)_{\pi zz}$ was found to have the strongest correlation.[19] However $NICS(1)_{zz}$ was also found to have a strong correlation and was recommended as a more readily computable alternative.

2.1.5 Isotropic shielding plots

Wolinski performed ab initio calculations to produce plots of magnetic shielding along axes through molecules by placing a neutron at regular positions along the axes.[20] The magnetic shielding values were calculated for the neutron, hence probing the magnetic shielding field at positions other than at the nuclei of the molecule in question. The work built on that by Johnson and Bovey who calculated NMR shifts at nuclei using a free electron model, but also hinted at the potential importance of off-nuclear magnetic shielding constants.[21] Indeed a significant amount of detail was observed including features which could not have been deduced by experiment alone. The positions of nuclei with non-zero nuclear magnetic spin being the only positions where it is currently possible to evaluate the magnetic shielding experimentally. Wolinski suggested that this was too restrictive and suggested off-nuclear shieldings could be of great use chemically. The work was limited to atoms and small linear molecules and determination of the isotropic shielding was done only along linear axes.

Kleinpeter and coworkers analysed the anisotropic effect in various functional groups such as double bonds and carbonyls through plots of the isotropic shielding.[22] The use of the anisotropic effect is important in conformational analysis where protons can be identified as being close to other functional groups, hence suitable conformations for the molecule can be predicted. They were able to categorize functional groups based on the intensity of the anisotropic effect and identify trends. Furthermore, from an analysis on the anisotropic effect on C-C bonds, it was found that the difference in chemical shift between equatorial and axial protons of cyclohexane was not predominantly due to the C-C anisotropy.[23]

Later Kleinpeter and coworkers formalized the procedure of calculating isotropic shielding at grid points throughout molecules to produce so-called iso-chemical shielding surfaces (ICSSs).[24] These were initially used to visually distinguish between aromatic and antiaromatic molecules. ICSSs were applied to many such relevant molecules including arenes, monosubstituted benzenes, ferrocene and annulenes. Forming such plots allowed comparison of the isotropic shielding values at all positions within a plane or cuboid, rather than just at positions frequently chosen to evaluate NICS. This allowed aromaticity to be determined by the characteristic shapes and patterns formed by these shielding values for aromatic and antiaromatic rings. They found that the ^{1}H NMR shifts calculated through their magnetic shielding data were largely in good agreement with experimental values therefore strengthening the validity of their ICSSs.

Karadakov and Horner also published contour and three-dimensional plots of isotropic shieldings sampled at various positions in order to evaluate aromaticity and antiaromaticity of molecules.[25] However, these plots used magnetic shielding sampled using a finer grid, 0.05 Å against 0.5 Å, making obvious the subtler details not seen in the ICSS plots. Their work on benzene and cyclobutadiene presented striking differences in magnetic shielding between these molecules (explained in detail later).[25] The technique was successfully employed to study the relative aromaticities of furan, pyrrole and thiophene where it reproduced the well-established order of aromaticity by careful study of how the isotropic shielding differs around the molecule.[26] Previous results through NICS alone, albeit at a smaller basis set of 6-31+G*, produced the wrong ordering of aromaticity for these molecules.[3]

In a recent paper the isotropic shielding plots were compared to the electron density plots for butadiene and showed significantly more detail.[27] Similar but non-identical bonds, such as C-H bonds in butadiene, could be readily distinguished which was not found to be the case with the electron density plots. In the electron density plots, bonds were represented by a drop in electron density between atoms whereas in the magnetic shielding plots bonds

could be seen as entities in themselves, being represented by tangible increases in magnetic shielding.

2.1.6 Atoms in molecules (AIM)

Bader developed the theory of Atoms in Molecules (AIM) in order to investigate molecular structure and reactivity by viewing the electron density as a scalar field thereby allowing manipulations frequently used in vector calculus and topology.[28] The theory was developed because attempts to interpret the electron charge density directly are difficult, especially due to the extreme values of charge density at the nuclei. The indirect method developed by Bader involves using the charge density as the potential for a gradient vector field. Bonds are defined via so called *bond paths* which connect nuclei and represent a path followed by gradient vectors where, at every point along this path, the electron density is a maximum in the plane perpendicular to the path. An atom in AIM is defined as a nucleus along with a so called *basin*, a subset of space surrounded by a surface for which there is zero flux of the gradient vector field.

The approach indicates that a gradient vector field formed from a scalar field can often indicate subtle details about the scalar field which are not immediately obvious. The isotropic shielding, being itself a scalar field, could also be analyzed in this way to further interpret the contour and three-dimensional plots obtained via quantum chemical calculations.

2.1.7 Aromaticity of the low-lying excited states of benzene and cyclobutadiene through magnetic evidence

Usings a variety of NICS indices, magnetic susceptibilities and carbon and proton shieldings Karadakov analysed the S_0, T_1 and S_1 states of benzene and the S_0, T_1, S_1 and S_2 states of square and rectangular cyclobutadiene in order to deduce their aromaticities.[29] In this paper CASSCF was used to include nondynamic correlation, a term for the electron correlation which is deficient in a single determinant wavefunction due to the electronic state not being well approximated by a single determinant. The following NICS indices were used: NICS(0), NICS(1), NICS$(0)_{zz}$ and NICS$(1)_{zz}$. No dissected NICS indices were used due to the lack, at the time of publication, of codes being available for dissected NICS using the CASSCF-GIAO technique.

The excited states of benzene appeared to have clearly categorizable aromaticities from NICS(0) data. The T_1 and S_1 states had NICS(0) values of 39.63 ppm and 45.81 ppm respectably, contrasting with the value of -8.17 ppm for the S_0 state. This suggests that the T_1 and S_1 states are antiaromatic, in contrast to the well known aromaticity of the S_0 state. Furthermore Karadakov went on to suggest that due to the relative magnitudes, the S_1 state

is a little more antiaromatic than the T_1 state. Similar conclusions can be drawn from the magnetic susceptibilities which were found to be -59.33 ppm cm^3 mol^{-1} for the S_0 state, with -6.16 and 2.43 for the T_1 and S_1 respectively, using the same units. The small magnitude of the magnetic susceptibilites for these latter two states suggest they antiaromatic. No data were published in this paper on the S_2 state of benzene.

The S_2 state of square cyclobutadiene produced a NICS(0) values of 22.10 ppm, and in comparison to the S_0 state, having a value of 36.41 ppm, it was concluded by Karadakov that the S_2 state was also antiaromatic but less so than the ground state. The T_1 and S_1 states of square cyclobutadiene produced the values -3.74 ppm and 3.44 ppm respectively hence are more troublesome to categorized as aromatic or antiaromatic. However it was argued that since both values are closer to the NICS(0) value for S_0 benzene than that of S_0 square cyclobutadiene, these two states are probably aromatic. The S_1 state being a rare example of a state with a positive NICS(0) value despite being most probably aromatic. In a similar line of reasoning to the T_1 and S_1 states of benzene, it was predicted that the S_1 state of cyclobutadiene is likely to be less aromatic than the T_1 state. This prediction is also supported by magnetic susceptibility data. The T_1 state has a value of -32.16 ppm cm^3 mol^{-1} which is more negative than that of the S_1 state at -28.78 ppm cm^3 mol^{-1}. The similarity of the states T_1 and S_1, seen in both benzene and cyclobutadiene, is a phenomenon also observed in cycloocta-1,3,5,7-tetraene (COT) where it was also found that these states have the opposite aromaticity to the ground state.[30]

Kataoka calculated magnetic susceptibilities for all singlet and triplet excited states of benzene up to S_3 and T_3.[31] It was concluded that the S_1 state, due to a large paramagnetism (a large negative magnetic susceptibility) is antiaromatic, as is the T_1 state. However the S_2 state is strongly diamagnetic and therefore is predicted to be aromatic. These results are very similar to those found by Karadakov, see above. Furthermore it is interesting to compare the values produced by the S_1 and T_1 states to attempt to predict relative aromaticity. The magnetic susceptibility value, as a unitless ratio of that for ground state benzene, for the S_1 state is -4.79 and that for T_1 is -2.00 potentially indicating that the S_1 state is more antiaromatic than the T_1 state.

2.1.8 Aromaticity of the low-lying excited states of benzene and cyclobutadiene through non-magnetic evidence

The use of well-established rules can provide strong indications that certain electronic states are likely to be aromatic or antiaromatic. Hückels rules are applied to ground states only and confirm the well known aromaticity of S_0 benzene and antiaromaticity of S_0 cyclobutadiene.

This is due to benzene having 4n+2 π-electrons, where n=1, and cyclobutadiene having 4n π-electrons, again where n=1.

Baird's rules can be applied in a similar manner to the lowest triplet state, and are defined as being the reversal of Hückels rules.[32] Therefore they indicate that the T_1 state of cyclobutadiene is aromatic due to the presence of 4n π-electrons, and that the T_1 state of benzene is antiaromatic due to the presence of 4n+2 π-electrons. This latter prediction is supported by experimental evidence where the T_1 state of benzene is shown to be unstable in the D_{6h} geometry with respect to a structure having D_{2h} symmetry.[33]

Soncini and Fowler introduced a set of rules based on ring current analyses which can be seen to build upon those introduced by Baird.[34] The rules state that annulenes with 4n+2 π-electrons in their lowest energy states with even total spin, and the annulenes of 4π-electrons in their lowest energy states of odd total spin will be aromatic. For the states of relevance to this text, these rules would indicate that the S_0 (S=0, hence even total spin) state of benzene would be aromatic, which is well known, and that the T_1 (S=1, hence odd total spin) state of cyclobutadiene would be aromatic too, which is already indicated by Bairds rules. However for analyses of electronic states of higher spin for these molecules the rules could produce interesting predictions, for instance that the lowest quintet state (S=2, even total spin) of benzene is also expected to be aromatic.

Fratev performed ab initio calculations on various excited states of cyclobutadiene, including all those analysed in this work.[35] Geometry optimizations found a D_{2h} geometry for the S_0 state, as expected, but found square D_{4h} geometries for all S_1, S_2 and T_1 states. Although the use of bond length equalization as a measure of aromaticity is considered unreliable, Fratev uses this as a primary criterion for aromaticity and therefore goes on to conclude that all these three low-lying excited states are not only less antiaromatic than the ground state, but suggests that they should most probably be aromatic.

2.2 Theory of magnetic shielding

When a circular wire is subjected to a magnetic field, current flows around the ring in order to create an induced magnetic field which opposes the external one, in a principle known as Lenz's law. A similar concept can be used to explain the production of an induced field by molecular rings with delocalized π-electrons. One indication that the molecular case is different from the macroscopic case is the peculiar behaviour that rings in the ground state containing 4π-electrons, hence antiaromatic, form paratropic currents which support the external field, whereas those containing 4n+2 π-electrons form diatropic currents which oppose the external field.

The paramagnetic currents are stronger than diamagnetic currents due to the dependence on their strengths on the HOMO-LUMO gap. Small HOMO-LUMO gaps are a well known feature of antiaromaticity, indeed these are smaller than those of aromatic molecules.[36] This is seen in practise where the NICS(0) values for antiaromatic molecules are generally much greater in magnitude than those of aromatic molecules.

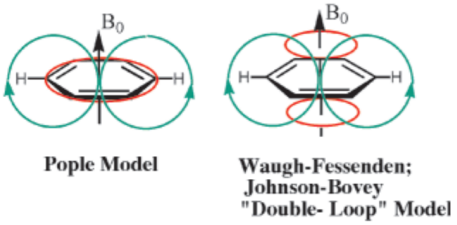

Figure 5: How the Pople and Double-Loop models predict a local magnetic field induced by ring currents. Image obtained from Ref [4]

In aromatic molecules the ring current produces a diamagnetic induced magnetic field which opposes the external field within the ring, but supports it outside. This is called the Pople model[37] and is illustrated in Figure 5. The additional magnetic field experienced by protons outside the ring leads to a downfield shift since the nuclei recieve the vector sum of the external and induced magnetic fields. For protons within the ring the induced field opposes the external one leading to an upfield shift for these nuclei.

The Pople model was improved upon by assuming that there were two rings of electrons, one above and one below the plane of the molecule, known as the double-loop model.[21;38] This was a refinement on the Pople model which improved its quantitative use. From analysis of π molecular orbitals it is immediately clear that electron density due to π-electrons is highest not in the plane, where the contribution is in fact zero, but above and below the plane. It was later suggested on the basis of $NICS_\pi$ values, that this model was inaccurate and that analyses produced no evidence for the presence of ring currents.[39]

2.3 Computational procedure

All calculations presented in this work used the CASSCF-GIAO method available in Dalton 2016.0[40] utilizing the MCSCF-GIAO methodology.[41;42]

CASSCF was chosen to include nondynamic correlation which was demonstrated to be important in determining accurate NICS values for antiaromatic states such as cyclobutadiene.[29] In contrast it was found that inclusion of electron correlation was far less significant in analysing the ground state aromaticity of benzene. Choosing a “6 in 6” CASSCF for benzene and a “4 in 4” CASSCF for cyclobutadiene allows the calculations to be done at a very similar qualitatively correct level of theory for both structures. The molecular geometries used in this paper are identical to those used in Ref [29].

Ghost atoms are structures, like atoms, which can be placed throughout a molecule within quantum chemistry software. They don't affect the wavefunction but can be used to probe quantities derived from the wavefunction at their locations. These were placed at all positions where the shielding tensors were to be calculated. These were placed in grids with a regular 0.05 Å spacing in both the two-dimensional contour plots and the three-dimensional isosurface plots. The square regions in the molecular plane was chosen to be 7 Å x 7 Å for benzene and 5 Å x 5 Å for cyclobutadiene with the perpendicular axis being 5 Å long for all three-dimensional plots for both molecules. The symmetry of the systems meant that only a portion of the space through a molecule needed to have isotropic shielding values calculated. Take a contour plot of benzene through the molecular plane as an example. Only one of the four quadrants needs to have isotropic shielding calculated as, by symmetry, the others will be identical. Therefore a region of 3.5 Å x 3.5 Å must be analysed and at a spacing of 0.05 Å this produced 71^2 ghost atoms. The values for this portion could then be reflected to the other four regions using a custom built FORTRAN program.

From work on the relative aromaticities of thiophene, pyrrole and furan, Karadakov and Horner concluded that the calculation of NICS benefited greatly by use of an extended basis set.[26] This was consided more important that the inclusion of dynamical electron correlation as introduced by the use of MP2 rather than HF. They came to this conclusion in part because the original NICS analysis of these molecules by Schleyer and coworkers[3] using HF-GIAO/6-31+G* failed to account for the well-established order of aromaticity whereas the use of the HF-GIAO/6-311++G(d,p) was able to reproduce this order. The use of MP2 rather than HF produced little improvement.

2.4 Results

2.4.1 Isotropic shielding plots applied to the benzene S_0 and cyclobutadiene S_0 states

Benzene S_0 and cyclobutadiene S_0 isotropic shielding data were originally produced and analysed by Karadakov and Horner in the CASSCF[6,6]/6-311++G(d,p) method and basis set producing contour plots and three-dimensional plots.[25] In the present work, using CASSCF[6,6]/6-311++G(2d,2p), plots were generated which were almost indistinguishable to those of this previous paper, therefore the same interpretation can be applied and is summarized as follows. The three-dimensional isovalue plots and two-dimensional contour plots produced in this work can be found in Figures 6 to 11.

Stark differences were observed in the overall appearence of the isotropic magentic shielding plots for the benzene S_0 and cyclobutadiene S_0, commonly seen as archetypal aromatic

and antiaromatic states respectively. Benzene S_0 was found to have a smooth torus-shaped shielding region passing through all carbon atoms in the ring, with additional protrusions of shielding reaching out towards the hydrogen atoms. Cyclobutadiene S_0, however, showed a large dumbell shaped region of deshielding through the centre of the ring, extending out perpendicular to the ring. Shielding regions were still observed encompassing the C-H bonds and the central regions of the C-C bonds, however these are punctured by the dumbell region which extends towards the deshielded regions around the carbon atoms.

The centre of the benzene S_0 ring was found to be only slightly positive, whereas the centre of the cyclobutadiene S_0 ring was strongly negative. This is due to the dumbell shape region of antiaromatic systems leading to far greater deshielding compared to the extent of shielding observed in aromatic systems, since there is no analogue of the dumbell shape for aromatic systems. Because antiaromaticity weakens the C-C bonds of the ring it was found that shielding regions between adjacent carbons were smaller in volume and reached lower maxima in cyclobutadiene S_0. It was also found that these regions have their maxima displaced towards the outside of the ring. The shielded regions around C-H bonds of the two states also highlight differences. These external bonds have weaker shielding in benzene S_0 than in cyclobutadiene S_0 indicating that the C-H bonds in the former might be weaker than the latter.

Characteristic features of the isotropic shielding plots for benzene S_0 and cyclobutadiene S_0, as archetypal aromatic and antiaromatic states respectively, can be used to deduce aromaticity and antiaromaticity in the other low-lying electronic states for these two molecules, and it is with this objective that the following results are presented and discussed.

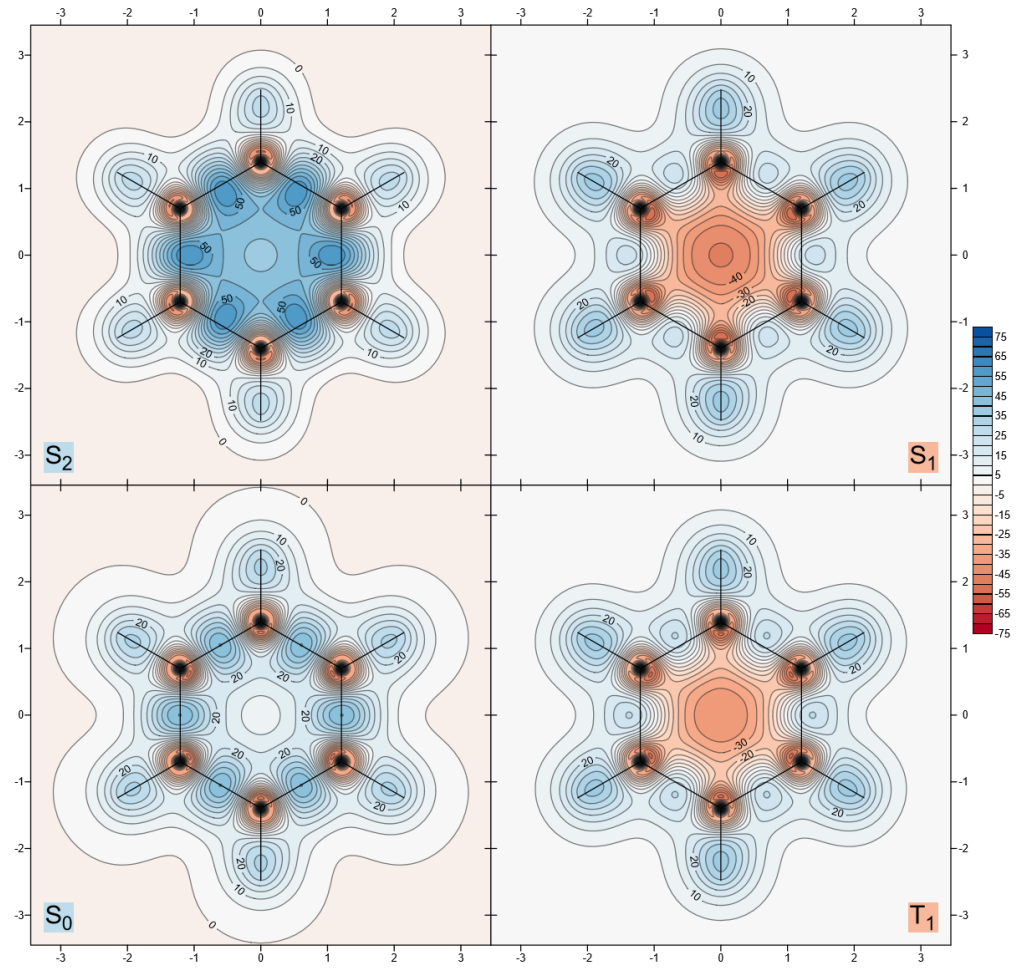

Figure 6: In-plane contour plots of the isotropic shielding for various electronic states of benzene. [5]

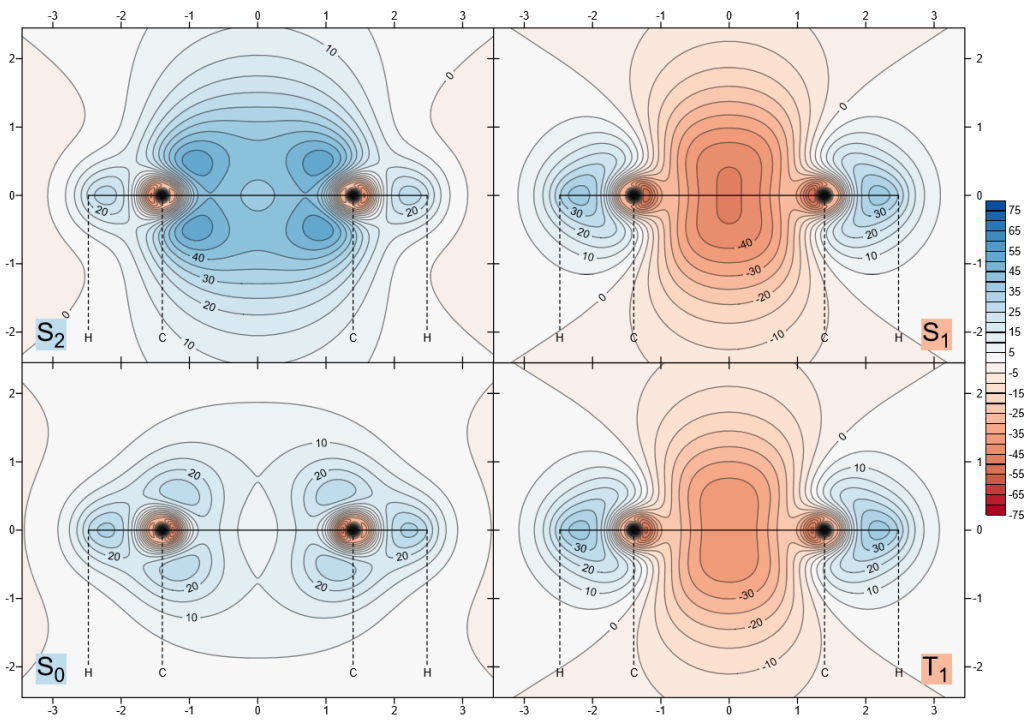

Figure 7: Through-atom perpendicular contour plots of the isotropic shielding for various electronic states of benzene. [5]

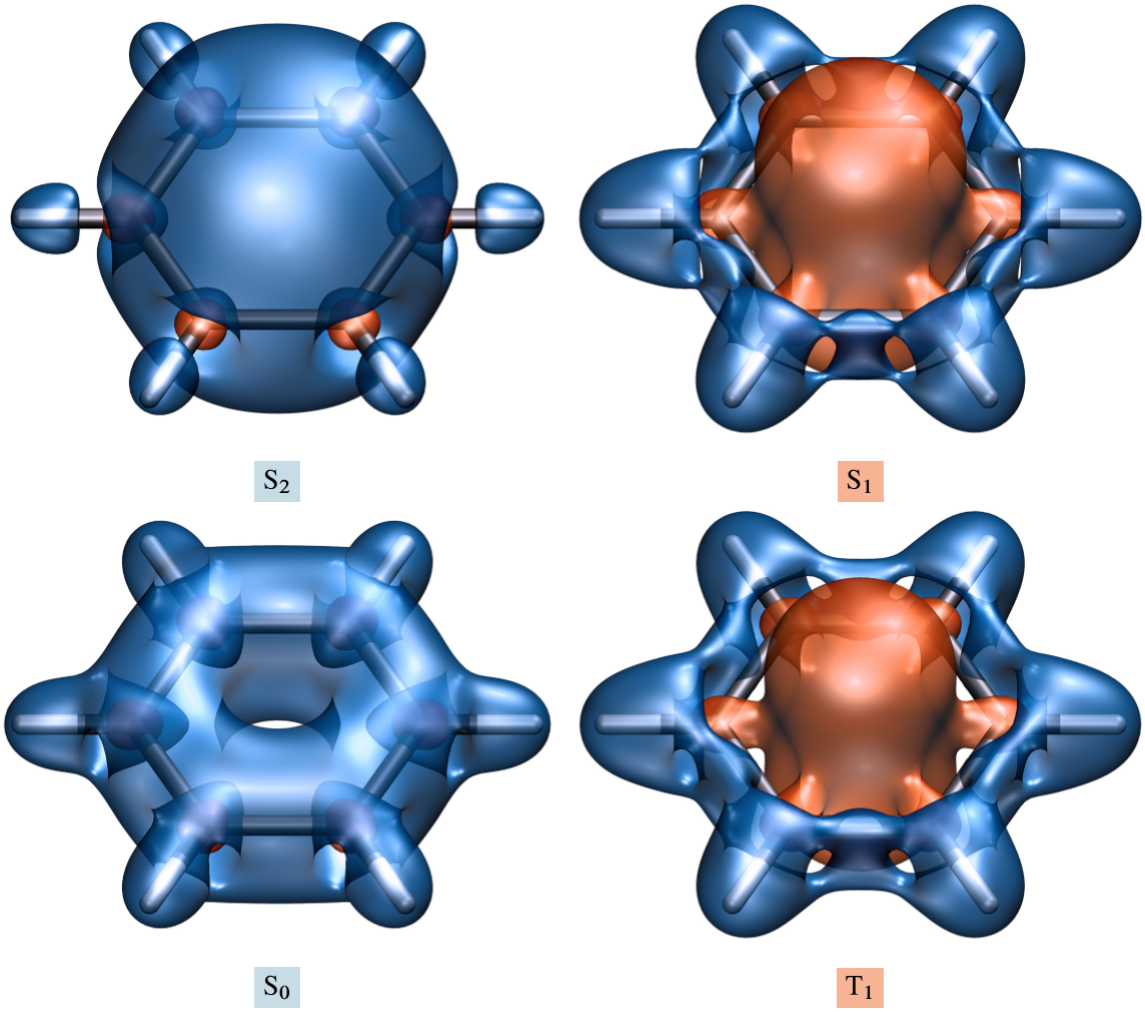

Figure 8: Three-dimensional isovalue plots of the isotropic shielding for various electronic states of benzene with isovalue ±16.[5]

2.4.2 Isotropic shielding plots applied to the benzene S_1 and T_1 states

The S_1 and T_1 states of benzene show a strong resemblence with antiaromatic cyclobutadiene S_0 having characteristic dumbell-shaped regions of deshielding present. The three-dimensional plots indicate how all three states have the vast majority of the ring region encompassed by deshielding with spurs connecting this region to the deshielding regions around each carbon. Furthermore a band of shielding can be seen to surround the ring encompassing the C-H bonds. Under the isovalue of ±16 in the three-dimensional plots both S_1 and T_1 states of benzene have very similar-looking shielding regions whereas this isovalue is too high to allow a continuous band to appear in the plot for S_0 cyclobutadiene.

Characteristic of antiaromatic states, the in-plane contour plots for the S_1 and T_1 states show lop-sided C-C bond shielded regions, whose maxima are displaced towards the outside of the ring. The maxima observed are 22.69 ppm for the S_1 state, 25.33 ppm for the T_1 state and these contrast to 24.38 ppm for S_0 cyclobutadiene. Also noticable from these plots is the extent of deshielding at the centre, reaching values which are far greater in magnitude, albeit

of opposite sign, than those at the centre of aromatic states such as benzene. At the centre NICS(0) values of 45.81 ppm and 39.63 ppm are reached for the S_1 and T_1 states respectively.

At first sight the T_1 state plots appear very similar to those of S_1. Both are clearly antiaromatic, however analysis indicates that the S_1 state is marginally more antiaromatic than the T_1 state. From the three-dimensional plots it can be seen that the deshielding dumbell is greater in the S_1 state than in the T_1 state. The in-plane plots exhibit a greater number of contour lines showing a greater build-up of deshielding at the centre of the ring for the S_1 state, which is further indicated by the NICS(0) values. The maximum C-C bond shielding of 25.33 ppm in the T_1 state compared to that of 22.69 ppm for the S_1 state indicates a lower level of antiaromaticity because there is less destabilization of the bonding framework. The ordering of the antiaromaticities of these two states is in agreement with both the NICS and magnetic susceptibility analyses reported in a previous section.

2.4.3 Isotropic shielding plots applied to the benzene S_2 state

The S_2 state shows a large region of shielding through the molecule, with the absence of the deshielded dumbell characteristic of antiaromaticity. However the three-dimensional plots indicate that this region is very different in appearance from that of the S_0 state, being more dome-shaped rather than a torus going through the carbons atoms of the ring. It is however observed that when the isovalue for this plot is raised to over ± 40 ppm the torus shape is observed. In this plot the central shielding region does not connect to the regions for each C-H bond, unlike the three-dimensional S_0 plot.

The in-plane contour plot shows that the shielding region reaches a minimum in magnitude at the centre of the ring, unlike the antiaromatic states which reach their maxima of deshielding at the centre point. However the NICS(0) value of -39.08 ppm is still large in magnitude. It is usually observed that the NICS(0) values for aromatic states are negative and small in magnitude, but those of antiaromatic states are positive and large in magnitude. This state is unusual for having a NICS(0) value whose magnitude is large enough for it to be comparable to that of antiaromatic states, despite being negative hence indicating aromaticity. A further indication of aromaticity from the in-plane contour plot is offered by the C-C bond shielding regions which are not triangular-shaped as they are in antiaromatic states. Nor are the maxima of these regions displaced towards the exterior of the ring, in fact they are markedly displaced inwards unlike any other electronic state analysed in this text. Furthermore these shielding regions reach a value of 59.74 ppm, far greater than that for benzene S_0 of 45.07 ppm.

The perpendicular contour plot shows just how much more shielding the S_2 state has than the S_0. However the main features are still present and further confirm this state as aromatic. These include the presence of small regions of especially strong shielding above and below each carbon tilted towards the centre. These can be seen to be especially strong for the S_2 state compared to S_0 benzene.

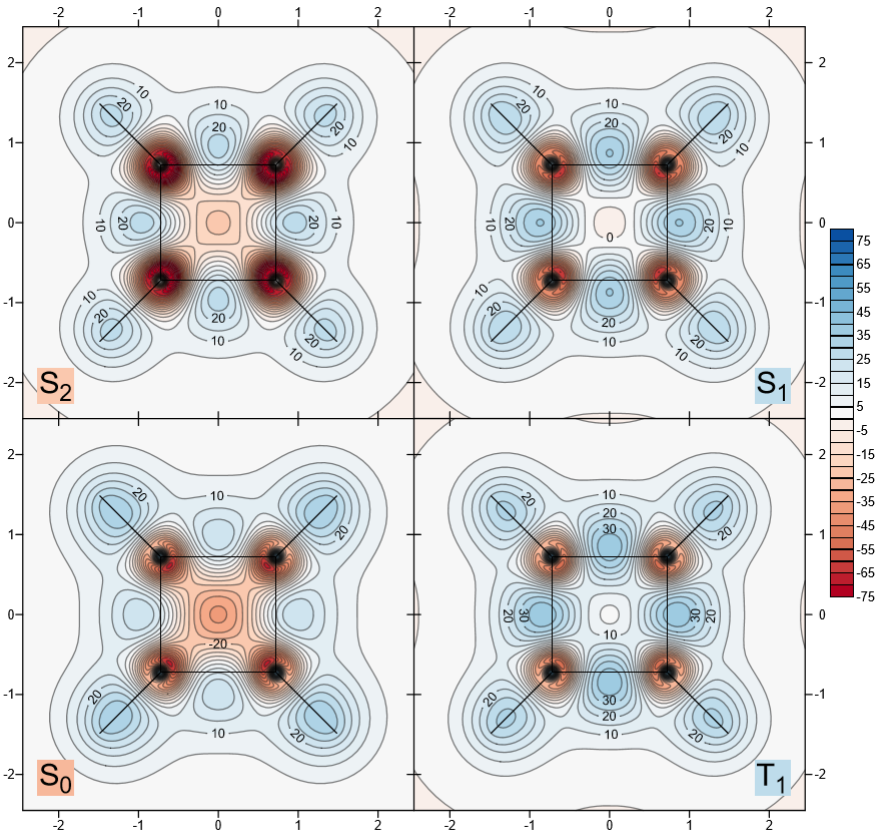

Figure 9: In-plane contour plots of the isotropic shielding for various electronic states of cyclobutadiene. [5]

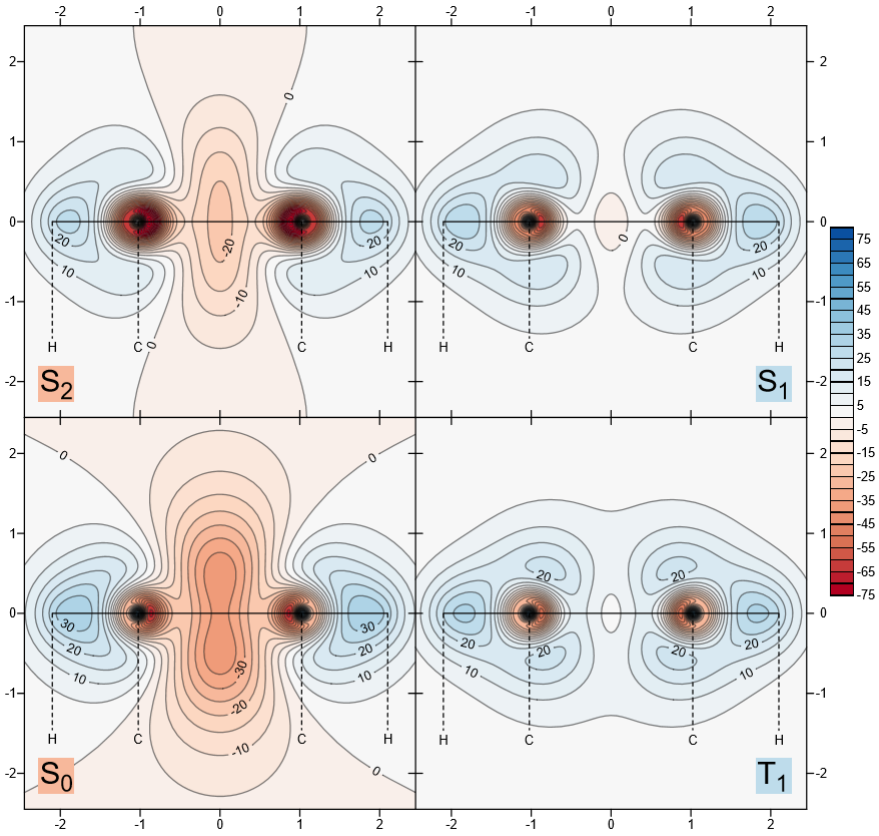

Figure 10: Through-atom perpendicular contour plots of the isotropic shielding for various electronic states of cyclobutadiene. [5]

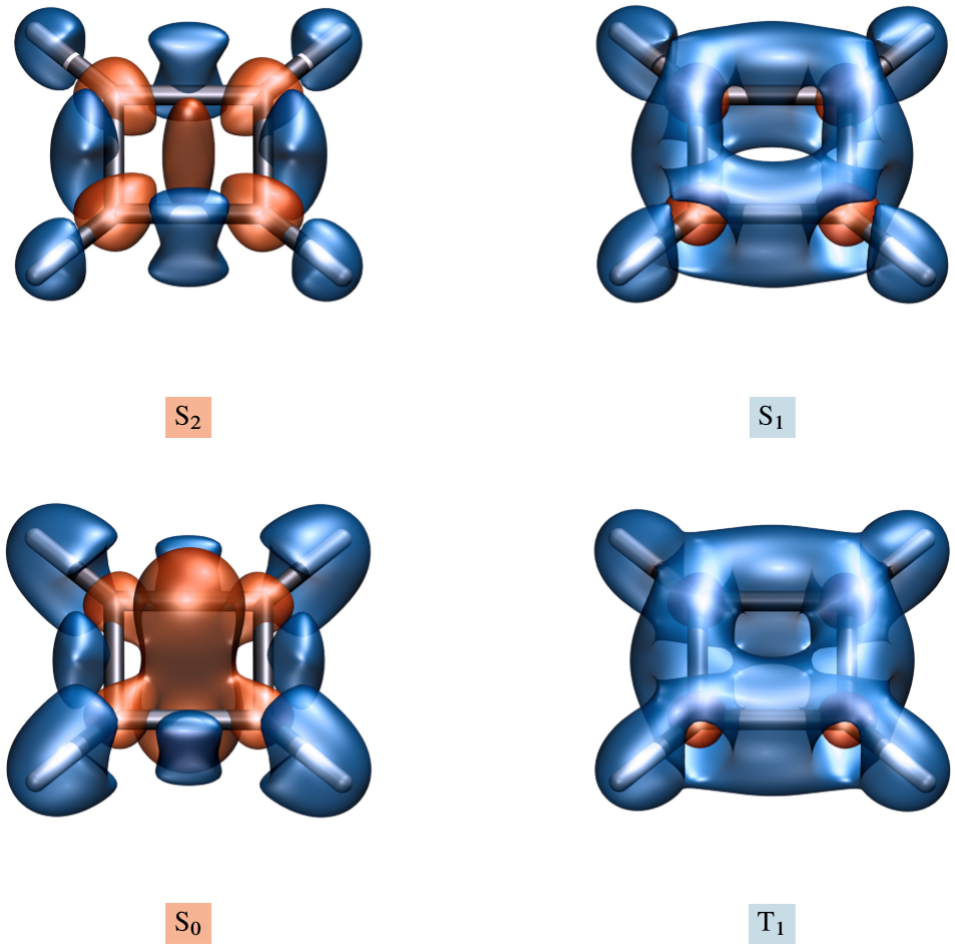

Figure 11: Three-dimensional isovalue plots of the isotropic shielding for various electronic states of cyclobutadiene with isovalue ±16.[5]

2.4.4 Isotropic shielding plots applied to the cyclobutadiene S_1 and T_1 states

The S_1 and T_1 states of cyclobutadiene appear very similar to the S_0 state of benzene, all of which feature a torus-shaped region of shielding encompassing the atoms of the ring. At the ring-centre of these states the isotropic shielding goes down to a value of low magnitude, in direct contrast with the large values present in antiaromatic states. In both the S_1 and T_1 states of cyclobutadiene and the S_0 state of benzene, the deshielding regions around each carbon are still observed and present themselves as punctures in the torus-shaped shielding regions. It can be seen from the three-dimensional plots that this puncturing is greatest in the S_1 state followed by the T_1 state of cyclobutadiene and least in the S_0 state of benzene. From the in-plane plots it can be seen that the C-C shielded regions are all roughly rectangular however marginally more lop-sided than the S_0 state of benzene. From these C-C regions it can also be seen that the maxima of the S_1 and T_1 states are displaced away from the midpoints between carbons, towards the exterior of the ring. The maxima of the shielding regions in S_0 benzene, in contrast, are directly at the midpoints between carbons. This feature

could be a result of the C-C bonds in cyclobutadiene being marginally more bent due to the tight bond angles.

An interesting feature of the S_1 state is that its NICS(0) value is positive, with a value of 3.44 ppm, despite the general appearance of the isotropic shielding being one of aromaticity. The in-plane contour plot shows this slight deshielding indicated by a pale red region at the centre of the molecule. Karadakov had previously assigned this state as aromatic due to the NICS(0) value being far closer to that of benzene than cyclobutadiene, as discussed in a previous section. The out-of-plane contour plots demonstrate no signs of a dumbell-shape for this small deshielded region. Through these plots it can be seen how minor this feature is compared to other features which unequivalently assign this state as aromatic.

Many features indicate the greater aromaticity of the T_1 state. The out-of-plane contour plots show that the shielding above and below the ring is greater for the T_1 state and that additional shielding is observed just above and below each carbon atom, tilted towards the ring, for the T_1 state. Larger maxima of 39.14 ppm for the C-C shielded regions is observed for the T_1 state in contrast to the value of 35.34 ppm for the equivalent maxima of the S_1 state. The higher NICS(0) value of 3.44 ppm of the S_1 state compared to the value of -3.74 ppm for the T_1 state is another indication of weaker aromaticity. On the basis of these features and the additional puncturing of the shielded region for the S_1 state it is concluded that there is a stronger aromaticity in the T_1 state.

2.4.5 Isotropic shielding plots applied to the cyclobutadiene S_2 state

The three-dimensional plots readily allow identification of the S_2 state as antiaromatic due to the immediate similarities with the S_0 plot. The deshielding dumbell at the centre of the ring is far weaker than that of the S_0 state, such that at the isovalue of ± 16 merging of this region with those around each carbon is not observed. It can also be seen that the C-H shielded regions present themselves as regions of smaller volume for the S_2 state in comparison with the S_0 state.

The in-plane plots show that the centre point of the ring is a local maximum in the magnitude of the deshielding reaching a NICS(0) value of 22.10 ppm in comparison with the value of larger magnitude of 36.41 ppm for the S_0 state. The C-C bonding regions also indicate that the S_2 state is of weaker antiaromaticity compared to the S_0 state. Maxima of these regions reach 27.97 ppm in the S_2 state compared to 24.38 ppm for the S_0 state, indicating stronger C-C bonds. It is immediately clear that the deshielded regions around each carbon are far greater deshielded for this state compared to the S_0 state and indeed any other state analysed in this text. This is an unusual feature because, for the features

previously mentioned, the S_2 state is considered less antiaromatic. Deshielded regions are observed around all sp^2 and sp carbons but no explanation for why this is has so far been put forward.

Perpendicular contour plots show how the central region has the correct shape for antiaromatic states but of far lower magnitude than that of the S_0 state. These plots also show how the C-H shielded regions reach maxima of 27.30 ppm, far lower than the equivalent values for other antiaromatic states: 34.62 ppm for S_0 cyclobutadiene, 37.03 ppm and 37.18 ppm for T_1 and S_1 benzene respectively. It is considered a feature of antiaromatic states to have greater shielding around the C-H bonds than for aromatic states. However the S_2 state has a value which is lower and more comparable to the values observed in aromatic states. One additional reason why this state could be considered unusual for antiaromatic states is that ab initio calculations have concluded that this excited state has a D_{4h} geometry, as mentioned earlier.

2.5 Conclusion

The results of this computational study conclude the S_0, S_2 states of benzene and the S_1, T_1 states of cyclobutadiene are aromatic and the S_1, T_1 states of benzene and the S_0, S_2 states of cyclobutadiene are antiaromatic. Several features were identified as markers for aromaticity and antiaromaticity hence allowing unambiguous classification. Aromaticity was marked by rectangular shielding regions for bonds within the ring, shielding positive and low magnitude at the centre of the ring and weak shielding regions for external bonds. Antiaromaticity was marked by weak lop-sided shielding regions for bonds within the ring, large dumbell-shaped region of deshielding extending above and below the molecular plane and strong shielding regions for external bonds.

Interestingly it was found that for both benzene and cyclobutadiene the first singlet excited state and the first triplet state were remarkably similar. It was found that the characteristic markers of aromaticity and antiaromaticity could build up sufficient evidence to state that in benzene the S_1 state was more antiaromatic than the T_1 state and in cyclobutadiene the T_1 state was more aromatic than the S_1 state. Previous classification by Karadakov had already reported this, but by noting several features in the plots of this research it was possible to state this more conclusively. The plots for the second singlet excited state for both molecules indicated that these had the same classification of aromatic or antiaromatic as the ground state, but differed in intensity. The S_2 state of benzene was considered more aromatic than the ground state largely because of a far greater shielding at the ring centre. The S_2 state of cyclobutadiene was unusual for a number of reasons described above, not least for its very

intense deshielded regions around each carbon. However enough evidence was present to classify this state as less antiaromatic than the ground state.

The singlet state alternation of aromaticity and antiaromaticity seen in these two molecules was also observed in cycloocta-1,3,5,7-tetraene (COT).[30] From this limited set of states for these three molecules it can be suggested that this may also be a property of annulenes in general or indeed other aromatic and antiaromatic molecules.

3 Exploring the possibility of non-orthogonal Boys localization

3.1 Introduction

Localized orbitals offer an alternative and equally valid electronic description to the use of traditional molecular orbitals, known as the canonical orbitals, which are produced in the Hartree-Fock method. Whereas canonical orbitals tend to be largely delocalized over the molecule, localized orbitals are spatially contracted. Both types of orbital have been helpful in reconciling quantum chemistry with traditional chemical concepts. For example canonical orbitals can be used to describe the relative probabilities of atoms within an allyl cation reacting with a nucleophile. An analysis of the low-lying LUMO shows that this orbital is composed primarily of orbitals on the carbons at either end of the molecule therefore predicting that nucleophilic attack occurs predominantly at these positions.[43] However for molecular systems without a great deal of electron delocalization, delocalized molecular orbitals can be difficult to interpret. For such systems localization offers an alternative which is often more similar to conventional understanding of molecules. For instance localized orbitals frequently resemble bonds and lone pairs. Furthermore since these orbitals depend predominantly on the local surroundings they can be used to describe the electronic structure of small sections of large molecules which are too big to be subjected to full ab initio calculations.

Localization typically occurs after a Hartree-Fock procedure when the canonical orbitals are known. Most localization procedures have associated functionals. Functionals are functions which have other functions as their arguments. In this case a localization functional depends on all the orbitals, which themselves are functions of position. By modifying the orbitals the value of the functional can be changed. Localization procedures involve optimizing functionals to maxima or minima by linear transformations of the canonical orbitals. In the case of the Boys functional, described later, the functional measures the sum of the spatial extensions of the orbitals hence is minimized to ensure localization.

Localization algorithms such as the Boys localization procedure include constraints to ensure orthogonality of resultant orbitals. This is used to ensure the orbitals remain linearly independent and are unable to converge into one another. Another reason is that integrals involving these orbitals are much simpler, for instance the matrix elements of Slater determinants include far fewer terms if the orbitals are orthogonal. However the constraint of orthogonality is not necessary to achieve a valid wavefunction and it is possible that the removal of this constraint would allow orbitals to be even more localized. The use of valence-bond theory has produced non-orthogonal orbitals which are considered largely localized and demonstrate localized features of the electronic structure of molecules.[44] The approach taken

in this text is to perform a traditional localization procedure, that of Boys localization, [18] using canonical orbitals but to remove the orthogonality constraint.

3.2 Orthogonal Boys localization

The following procedure is an adapted version of that presented in Ref [17]. The Boys procedure involves the minimization of the Boys functional, Eq. (32). [18]

$$B\{\phi_i\} = \sum_{i=1}^{N} \langle ii|(\mathbf{r}_1 - \mathbf{r}_2)^2|ii\rangle \tag{32}$$

where N is the number of occupied molecular orbitals, excluding core orbitals if these are not to be involved in the localization.

The equations in this form are difficult to solve but the Boys functional can be rewritten in terms of one-electron rather than two-electron integrals.

$$B\{\phi_i\} = -\frac{2}{N} G\{\phi_i\} + 2Tr(\mathbf{r}^2) - \frac{2}{N}(Tr(\mathbf{r}))^2 \tag{33}$$

$$G\{\phi_i\} = \sum_{i=1}^{N} \sum_{j=i+1}^{N} (\langle j|\mathbf{r}|j\rangle - \langle i|\mathbf{r}|i\rangle)^2 \tag{34}$$

where we shall call the functional $G\{\phi_i\}$ the Boys sub-functional.

Since the localization is a transformation from an orthonormal set (the canonical orbitals) to another orthonormal set (the Boys orbitals), it is represented by a unitary transformation.

$$|j'\rangle = \sum_i U_{ij}|i\rangle \tag{35}$$

where U is the transformation matrix whose columns are the linear combinations of the canonical orbitals which make up the Boys localized orbitals.

It is a well-known result of linear algebra that the trace of any operator is preserved under a similarity, which includes unitary, transformation. Therefore through optimization of this functional the latter two terms of Eq. (33) will be constant. The problem then becomes one of finding a unitary transformation which equivalently minimizes the Boys functional and maximizes the double summation i.e. the Boys sub-functional.

The integral $\langle j|\mathbf{r}|j\rangle$ is known as the *orbital centroid* for orbital ϕ_i. This is a three-dimensional

vector considered to represent the centre of the orbital. The double summation can therefore be seen as the sum of the squares of distances between centroids of all unique pairs of orbitals. Since this summation is to be maximized, the problem is to find a set of orbitals such that the centroids are separated as much as possible.

The problem can be solved by a 2x2 rotation algorithm first introduced by Edmiston and Ruedenberg.[45;46] The procedure is to cycle through all unique pairs of orbitals at a time and apply a 2x2 rotation with an angle which is to be determined.

$$\begin{pmatrix} |\phi'_a\rangle \\ |\phi'_b\rangle \end{pmatrix} = \begin{pmatrix} \cos\gamma & \sin\gamma \\ -\sin\gamma & \cos\gamma \end{pmatrix} \begin{pmatrix} |\phi_a\rangle \\ |\phi_b\rangle \end{pmatrix} \tag{36}$$

The sets $\{|\phi'_i\rangle\}$ and $\{|\phi_i\rangle\}$ are identical with the sole exception of the above alterations to orbitals ϕ_a and ϕ_b. It is possible to express the value of $B\{\phi'_i\}$ in terms of $B\{\phi_i\}$ and thereby deduce the value of γ which minimizes $B\{\phi'_i\}$. A replacement of $\{|\phi_i\rangle\}$ with $\{|\phi'_i\rangle\}$ allows the procedure to continue by selecting another pair of orbitals and performing a similar minimizing rotation with these. Rotation matrices are necessarily unitary and a product of unitary matrices is itself unitary. This implies that the transformation matrix, which is the result of this succession of 2x2 rotations, will itself be unitary therefore the resulting localized orbitals will be orthonormal.

A possible convergence criterion is to stop the algorithm when the minimizing values of γ for all pairs are below a threshold value in magnitude. There is no guarantee that this procedure of successive rotations will converge to a solution. In practice convergence is usually observed although may require many hundred of such rotations.

3.3 Non-orthogonal Boys localization

The aim of this research was to minimize the Boys functional constrained only insofar as the resultant orbitals remain normalized. In order to do this a test system was chosen and all subsequent calculations performed with it. This was the RHF molecular orbitals (MOs) of water, of which there are five. It is common in localization to keep core orbitals frozen, therefore four MOs were relevant to the localization. A transformation matrix of four canonical MOs to four localized MOs would be a 4x4 matrix, containing 16 parameters. If we had the constraint of orthogonality we would require this transformation matrix to be unitary. Instead we wish to ensure linear independence which is equivalent to ensuring the transformation matrix is a member of the general linear group of order four, the group of all 4x4 matrices with non-zero determinant. The equation describing the transformation is given by Eq. (37).

$$|j'\rangle = \sum_i X_{ij}|i\rangle \tag{37}$$

where X is the transformation matrix, $\{|\phi_i'\rangle\}$ is the set of localized orbitals and $\{|\phi_i\rangle\}$ is the set of canonical orbitals.

Each of the four localized MOs must remain normalized, hence introducing four equality constraints, Eq. (38), reducing the number of variational parameters to 12. The problem is now one of unconstrained minimization of the Boys functional over these 12 parameters.

$$\langle i'|i'\rangle = 1 = \sum_j \sum_k X_{ji}^* X_{ki} \langle j|k\rangle \text{ for } i = 1, \ldots, 4 \tag{38}$$

A significant problem with non-orthogonal localization is that no constraint is present to prevent orbitals from converging into one another. The problem with this self-convergence is that it would result in a Slater determinant wavefunction being identically zero because two columns would be equal. It was theorized that since minimization of the Boys functional inherently attempts to separate orbital centroids, it was possible that the unconstrained minimization could lead to linearly independent localized orbitals. It was shown earlier that the minimization of the Boys functional is equivalent to maximizing the Boys sub-functional, $G\{\phi_i\}$.

$$G\{\phi_i\} = \sum_{i=1}^{N} \sum_{j=i+1}^{N} \left(\langle j|\mathbf{r}|j\rangle - \langle i|\mathbf{r}|i\rangle\right)^2 \tag{34}$$

This functional is based on the sum of squares of distances between orbital centroids. In maximizing this, the orbitals would naturally attempt to spread apart so as to increase the distances between orbital centroids, and hence increase the sum of squares of distances. Widely separated orbitals would not be subject to the problem appearing when orbitals converge into one another and hence become linearly dependent.

3.4 Algorithm and computational procedure

Aside from common techniques of optimization which could yield solutions, such as Lagrange multipliers, derivative-based methods and quadratic programming, a method based on systematic scanning of the parameter space was chosen. The reason for this was because it's the easiest method to implement and test. Although the computational cost of this method scales poorly with system size this is not a problem because initially it is to be applied only to small molecules as a means of testing the localization.

It was believed that the solutions to the minimization of the Boys functional without orthogonality constraints would appear similar in form to those produced by standard means. Therefore the 4x4 transformation matrix was chosen to be written in the basis of the four orthogonal Boys localized orbitals so that the minimizing transformation matrix was most likely to be a small perturbation on the identity matrix.[1] The identity matrix being the transformation matrix which would reproduce the orthogonal Boys localized orbitals. In order to put the four equality constraints into practice, intermediate normalization was used. The diagonal elements were fixed at values of one, whilst all other matrix elements could be varied. The choice of intermediate normalization rested on the assumption that the off-diagonal elements would be small in magnitude. Before the Boys functional value could be calculated from a given transformation matrix, it is necessary that the columns of the transformation matrix must then be scaled, so as to ensure strict normalization of the resulting orbitals.

Having fixed the four diagonal matrix elements, the remaining 12 were parameters to be varied. The procedure involved selecting a set of possible values for each parameter, examples shown in Table 1 consisting of nine values per set. The program would form every possible transformation matrix for all combinations of parameters and their possible values. For a set of nine possible values, the number of such matrices was $9^{12} = 2.82\text{x}10^{11}$. The programming technique of recursion was utilized to efficiently scan through these matrices. The program source code is available in Appendix B.

Each transfomation matrix would be formed, normalized, then the Boys functional value calculated for the resulting localized orbitals. The program recorded ten transformation matrices which attained the highest Boys sub-functional values. Even if many attained the same Boys sub-functional value, all would be included.

Although the variational parameters had only fixed values for which they could attain the value of, it was hoped that these were sufficient to scan the parameter space and predict what sort of transformation matrix would solve the global optimization problem. A greater number of possible values would increase the accuracy of the optimization but would also rapidly increase the computational expense. Although the time taken for each run, consisting of nine possible values, would depend on the computational resources available, these calculations can be expected to take a number of days each.

[1]Note here the term basis is used as it is in linear algebra rather than the more applied meaning of the term basis sets in quantum chemistry. The mathematical term is defined for a given vector space as a minimal subset whose span reproduces the vector space.

Table 1: Set of possible parameter values for each run of the program

Run 1	-5.00	-1.00	-0.50	-0.25	0.00	0.25	0.50	1.00	5.00
Run 2	-0.70	-0.50	-0.30	-0.10	0.00	0.10	0.30	0.50	0.70
Run 3	-10.00	-5.00	-1.00	-0.50	0.00	0.50	1.00	5.00	10.00

3.5 Results

3.5.1 Run 1 : Balanced range of parameter values

A wide range of permitted values, over several runs, were chosen and their values presented in Table 1. Run 1 was an initial application of the program, using parameter values of row 1 in this table, to scan both small and large values to determine the sort of matrix which produces large values of the Boys sub-functional. Producing a value of 17.0620, the results were considered very interesting on the account that the orthogonal Boys orbitals themselves produced a value of 14.57. Hence we have shown that localized orbitals can be designed, which aren't constrained to be orthogonal, to produce a greater value for the Boys sub-functional than the traditional orthogonal Boys orbitals. This equivalently means a lower minimum of the Boys functional itself.

In total four matrices, from those possible in Run 1 attained this maximal value of the Boys sub-functional. All of which contained a parameter holding the maximum value permitted, which in this run was 5.0. This seemed contrary to the prediction that a maximum of the Boys functional would produce a transformation matrix which was only a small perturbation on the identity matrix. To investigate this further, two additional runs were performed. The second run investigates small values of the parameters, up to a magnitude of 0.7. This was chosen to investigate whether large values of the Boys sub-functional were possible for localized orbitals which were only marginally perturbed from the orthogonal Boys orbitals. The third run investigated the other extreme, and had a selection of permitted values which reached 10.0 in magnitude. This was primarily to determine whether our initial prediction that the non-orthogonal Boys localized orbitals would be similar in form to the orthogonal Boys localized orbitals. If the largest Boys functional values were attained for matrices containing parameters holding the values 10.0 or -10.0, this would strongly suggest that the global solution to the non-orthogonal Boys localization problem could not be achieved by a small modification on the orthogonal Boys localized orbitals. The optimal matrices and associated Boys sub-functional values for all three runs are presented in Appendix A.

3.5.2 Run 2 : Contracted range of parameter values

Run 2, utilizing parameter values of row 2 in Table 1, produced a maximum Boys sub-functional value of 15.8601. There was only one matrix which attained this value, although

two which attained the similar value 15.8519. This maximizing matrix was surprising because it contained only parameter values of magnitudes 0.0, 0.1 and 0.3, despite the larger values of 0.5 and 0.7 being available. This is in contrast to Run 1 for which all matrices attaining the maximum value contained the maximum parameter value of 5.0. The value 15.8601 is therefore considered to be close to that of a local maximum, or saddle-point, which could be found exactly via derivative based methods. This result must certainly not be a global maximum due to the existence of a matrix producing the greater value of 17.0620 found in Run 1.

3.5.3 Run 3 : Extended range of parameter values

Run 3, utilizing parameter values of row 3 in Table 1, produced a maximum Boys functional value of 17.1854. A total of four matrices produced this value in the scan. This value is greater than that of Run 1 suggesting that this uses a better set of parameter values to perform the scan with. Interestingly this Boys functional value is attained with matrices all containing a significant number of parameters with the value 10.0 or -10.0 in direct contradiction of the prediction that the Boys functional would be maximized using a matrix being only a small perturbation on the identity matrix.

3.6 Discussion

The results have indicated that achieving the largest Boys sub-functional value requires the use of large parameters. This implies that the exact solutions, transformation matrix or matrices which achieve a maximum of the Boys sub-functional, will produce a set of orbitals with some significant differences to the set produced by an orthogonal Boys procedure. Interestingly there appears to be a local maximum or saddle-point similar in form to the orthogonal Boys localized orbitals as revealed by Run 2, however the objective is to achieve a global maximum therefore this feature will not be discussed further.

Table 2: First matrix in program output for Run 3, see Appendix A

1.00	0.00	0.00	0.00	0.00
0.00	1.00	-10.00	0.00	10.00
0.00	10.00	1.00	10.00	0.00
0.00	1.00	-1.00	1.00	1.00
0.00	1.00	-1.00	1.00	1.00

The first matrix which appears in the list of those attaining the highest value of the Boys sub-function in Run 3 is presented in Table 2. The other matrices which attain this highest value are very similar, differing predominantly in the arrangement of columns. In order to

investigate what sort of transformation matrices and hence sets of orbitals are attaining the highest values of the Boys sub-functional we analyse this matrix as an example. Firstly it can be seen that this matrix is strictly linearly independent because for each column, no linear combination of the remaining columns can produce that column. However the matrix is weakly linearly independent because linear combinations of other columns can produce a vector similar to the chosen column. In this matrix it can be seen that columns 3 and 5 are almost the negative of one another. Likewise columns 2 and 4 are almost the same. It is important to note that after normalization all components for each column will be scaled down so all components of magnitude one will actually contribute a far smaller magnitude to that orbital. It is interesting to see that the orbitals corresponding to columns 2 and 4 will appear similar in form to the third orthogonal Boys orbital and that the orbitals corresponding to columns 3 and 5 will appear similar in form to the second orthogonal Boys orbital. The use of values of unity along the diagonal was designed to prevent orbitals from turning into one another. However this only works if the permitted parameter values are small. As can be seen in this example large parameter values permit a dwarfing of these fixed diagonal values allowing them to become almost insignificant after normalization.

Although normalization has been accounted for in the algorithm, no attempt to encourage linear independence has been implemented. Linear independence is assured by the use of orthogonality, however without orthogonality there can be no guarantee of linear independence. It was thought possible that linear independence would occur naturally in the procedure due to separation of orbitals which occurs through maximization of the Boys sub-functional (see above for greater detail). With the above results it now appears that the natural separation of the algorithm is not generally sufficient in ensuring complete linear independence.

The algorithm strongly appears to be converging towards a solution which would either be linearly dependent or minutely linearly independent (which would be accompanied by an overlap integral of pairs of orbitals approaching a value close to unity). This converged solution would be achieved if the parameters were freely variable.

3.7 Conclusion

The results strongly suggest that there can be no generally-applicable non-orthogonal Boys procedure which omits any sort of constraint on linear independence. It is possible that such a procedure would successfully optimize to linearly independent orbitals for a system other than the water molecule. The conclusion applied to the water molecule holds because the domain over which the optimization is performed has been thoroughly scanned. Allowing parameter values to reach greater magnitudes has allowed the Boys sub-functional to reach greater maxima through a convergence of orbitals into one another.

In order to produce non-orthogonal localized orbitals there are two possible modifications which can be applied. Firstly the Boys functional could be retained and constraints which ensure linear independence included in the optimization. Secondly the functional itself could be altered, and optimization remain unconstrained with the exception of normalization.

On the problem of linear independence constraints, the application of such a constraint is hindered by the fact that an arbitrarily small modification can turn a set of orbitals from linearly dependent to independent. If indeed the true minimum of the Boys localization problem is a set of linearly dependent orbitals, then a minute change in the coefficients can lead this set to be linearly independent. However such a minute modification of the coefficients will lead to orbitals which, for all practical purposes are the same, despite technically being linearly independent, which is clearly an insufficient solution. Such a constraint can be compared to a trivial problem of minimization of a function $f(x) = x$ subject to the constraint that $x > 0$. Due to the strict inequality constraint there is no solution to this problem but we can get infinitesimally close by reducing x down to almost zero without ever reaching it.

A more promising solution is to change the functional which is used to produce the localized orbitals. The functional could include a repulsion of centroids strong enough to ensure that optimization of the functional can never produce mutually converging orbitals. This would avoid the need for a constraint to ensure the orbitals don't become linearly dependent. Although a program like the one used in this text could indicate the rough form of the solution there are almost always quicker and more accurate optimization procedures which can be used on a given functional. Newton-type optimization is one such example which would allow simultanous optimization of all variational parameters, assuming the derivative can be readily calculated with respect to each of these parameters.

A Appendix A

Program output for Run 1

```
RANK  1
  17.0620
 Matrix X
     1.00     0.00     0.00     0.00     0.00
     0.00     1.00     0.00     0.00     5.00
     0.00     0.00     1.00     5.00     0.00
     0.00     0.00     0.25     1.00     0.50
     0.00     0.25     0.00     0.50     1.00
 Matrix <i'|x|i'>/<i'|i'>
   0.0000
   0.8655
  -0.8655
  -0.8882
   0.8882
 Matrix <i'|y|i'>/<i'|i'>
  -0.0000
   0.1251
  -0.1251
  -0.0530
   0.0530
 Matrix <i'|z|i'>/<i'|i'>
  -0.1236
   0.4889
   0.4889
   0.4877
   0.4877
RANK  2
  17.0620
 Matrix X
     1.00     0.00     0.00     0.00     0.00
     0.00     1.00     0.00     0.00     5.00
     0.00     0.00     1.00     5.00     0.00
     0.00     0.25     0.00     1.00     0.50
     0.00     0.00     0.25     0.50     1.00
```

```
 Matrix <i'|x|i'>/<i'|i'>
   0.0000
   0.8655
  -0.8655
  -0.8882
   0.8882
 Matrix <i'|y|i'>/<i'|i'>
  -0.0000
  -0.1251
   0.1251
  -0.0530
   0.0530
 Matrix <i'|z|i'>/<i'|i'>
  -0.1236
   0.4889
   0.4889
   0.4877
   0.4877
RANK  3
  17.0620
 Matrix X
     1.00     0.00     0.00     0.00     0.00
     0.00     1.00     0.00     5.00     0.00
     0.00     0.00     1.00     0.00     5.00
     0.00     0.25     0.00     1.00     0.50
     0.00     0.00     0.25     0.50     1.00
 Matrix <i'|x|i'>/<i'|i'>
   0.0000
   0.8655
  -0.8655
   0.8882
  -0.8882
 Matrix <i'|y|i'>/<i'|i'>
  -0.0000
  -0.1251
   0.1251
  -0.0530
```

```
   0.0530
 Matrix <i'|z|i'>/<i'|i'>
  -0.1236
   0.4889
   0.4889
   0.4877
   0.4877
RANK  4
  17.0620
 Matrix X
     1.00     0.00     0.00     0.00     0.00
     0.00     1.00     0.00     5.00     0.00
     0.00     0.00     1.00     0.00     5.00
     0.00     0.00     0.25     1.00     0.50
     0.00     0.25     0.00     0.50     1.00
 Matrix <i'|x|i'>/<i'|i'>
   0.0000
   0.8655
  -0.8655
   0.8882
  -0.8882
 Matrix <i'|y|i'>/<i'|i'>
  -0.0000
   0.1251
  -0.1251
  -0.0530
   0.0530
 Matrix <i'|z|i'>/<i'|i'>
  -0.1236
   0.4889
   0.4889
   0.4877
   0.4877
RANK  5
  17.0399
 Matrix X
     1.00     0.00     0.00     0.00     0.00
```

```
     0.00     1.00     0.00     0.00     5.00
     0.00     0.00     1.00     5.00     0.00
     0.00     0.00     0.25     1.00     0.50
     0.00     0.25     0.00     0.25     1.00
 Matrix <i'|x|i'>/<i'|i'>
   0.0000
   0.8655
  -0.8655
  -0.8821
   0.8882
 Matrix <i'|y|i'>/<i'|i'>
  -0.0000
   0.1251
  -0.1251
  -0.0765
   0.0530
 Matrix <i'|z|i'>/<i'|i'>
  -0.1236
   0.4889
   0.4889
   0.5007
   0.4877
RANK  6
  17.0399
 Matrix X
     1.00     0.00     0.00     0.00     0.00
     0.00     1.00     0.00     0.00     5.00
     0.00     0.00     1.00     5.00     0.00
     0.00     0.00     0.25     1.00     0.25
     0.00     0.25     0.00     0.50     1.00
 Matrix <i'|x|i'>/<i'|i'>
   0.0000
   0.8655
  -0.8655
  -0.8882
   0.8821
 Matrix <i'|y|i'>/<i'|i'>
```

```
 -0.0000
  0.1251
 -0.1251
 -0.0530
  0.0765
 Matrix <i'|z|i'>/<i'|i'>
 -0.1236
  0.4889
  0.4889
  0.4877
  0.5007
RANK  7
 17.0399
 Matrix X
    1.00     0.00     0.00     0.00     0.00
    0.00     1.00     0.00     5.00     0.00
    0.00     0.00     1.00     0.00     5.00
    0.00     0.00     0.25     1.00     0.50
    0.00     0.25     0.00     0.25     1.00
 Matrix <i'|x|i'>/<i'|i'>
  0.0000
  0.8655
 -0.8655
  0.8821
 -0.8882
 Matrix <i'|y|i'>/<i'|i'>
 -0.0000
  0.1251
 -0.1251
 -0.0765
  0.0530
 Matrix <i'|z|i'>/<i'|i'>
 -0.1236
  0.4889
  0.4889
  0.5007
  0.4877
```

```
RANK  8
  17.0399
 Matrix X
     1.00     0.00     0.00     0.00     0.00
     0.00     1.00     0.00     5.00     0.00
     0.00     0.00     1.00     0.00     5.00
     0.00     0.00     0.25     1.00     0.25
     0.00     0.25     0.00     0.50     1.00
 Matrix <i'|x|i'>/<i'|i'>
   0.0000
   0.8655
  -0.8655
   0.8882
  -0.8821
 Matrix <i'|y|i'>/<i'|i'>
  -0.0000
   0.1251
  -0.1251
  -0.0530
   0.0765
 Matrix <i'|z|i'>/<i'|i'>
  -0.1236
   0.4889
   0.4889
   0.4877
   0.5007
RANK  9
  17.0399
 Matrix X
     1.00     0.00     0.00     0.00     0.00
     0.00     1.00     0.00     0.00     5.00
     0.00     0.00     1.00     5.00     0.00
     0.00     0.25     0.00     1.00     0.50
     0.00     0.00     0.25     0.25     1.00
 Matrix <i'|x|i'>/<i'|i'>
   0.0000
   0.8655
```

```
 -0.8655
 -0.8821
  0.8882
Matrix <i'|y|i'>/<i'|i'>
 -0.0000
 -0.1251
  0.1251
 -0.0765
  0.0530
Matrix <i'|z|i'>/<i'|i'>
 -0.1236
  0.4889
  0.4889
  0.5007
  0.4877
RANK 10
 17.0399
Matrix X
    1.00     0.00     0.00     0.00     0.00
    0.00     1.00     0.00     0.00     5.00
    0.00     0.00     1.00     5.00     0.00
    0.00     0.25     0.00     1.00     0.25
    0.00     0.00     0.25     0.50     1.00
Matrix <i'|x|i'>/<i'|i'>
  0.0000
  0.8655
 -0.8655
 -0.8882
  0.8821
Matrix <i'|y|i'>/<i'|i'>
 -0.0000
 -0.1251
  0.1251
 -0.0530
  0.0765
Matrix <i'|z|i'>/<i'|i'>
 -0.1236
```

0.4889

0.4889

0.4877

0.5007

Program output for Run 2

```
RANK  1
  15.8601
 Matrix X
     1.00     0.00     0.00     0.00     0.00
     0.00     1.00     0.10     0.10     0.10
     0.00     0.10     1.00     0.10     0.10
     0.00     0.10     0.10     1.00     0.30
     0.00     0.10     0.10     0.30     1.00
 Matrix <i'|x|i'>/<i'|i'>
   0.0000
   0.8670
  -0.8670
   0.0000
   0.0000
 Matrix <i'|y|i'>/<i'|i'>
  -0.0000
  -0.0000
   0.0000
  -0.4583
   0.4583
 Matrix <i'|z|i'>/<i'|i'>
  -0.1236
   0.5572
   0.5572
  -0.5546
  -0.5546
RANK  2
  15.8519
 Matrix X
     1.00     0.00     0.00     0.00     0.00
     0.00     1.00     0.10     0.10     0.10
     0.00     0.00     1.00     0.10     0.10
     0.00     0.10     0.10     1.00     0.30
     0.00     0.10     0.10     0.30     1.00
 Matrix <i'|x|i'>/<i'|i'>
   0.0000
```

```
  0.8889
 -0.8670
  0.0000
  0.0000
 Matrix <i'|y|i'>/<i'|i'>
 -0.0000
 -0.0000
  0.0000
 -0.4583
  0.4583
 Matrix <i'|z|i'>/<i'|i'>
 -0.1236
  0.5218
  0.5572
 -0.5546
 -0.5546
RANK  3
  15.8519
 Matrix X
     1.00     0.00     0.00     0.00     0.00
     0.00     1.00     0.00     0.10     0.10
     0.00     0.10     1.00     0.10     0.10
     0.00     0.10     0.10     1.00     0.30
     0.00     0.10     0.10     0.30     1.00
 Matrix <i'|x|i'>/<i'|i'>
  0.0000
  0.8670
 -0.8889
  0.0000
  0.0000
 Matrix <i'|y|i'>/<i'|i'>
 -0.0000
 -0.0000
  0.0000
 -0.4583
  0.4583
 Matrix <i'|z|i'>/<i'|i'>
```

```
  -0.1236
   0.5572
   0.5218
  -0.5546
  -0.5546
RANK  4
  15.8482
 Matrix X
     1.00     0.00     0.00     0.00     0.00
     0.00     1.00     0.10     0.10     0.10
     0.00     0.10     1.00     0.10     0.10
     0.00     0.10     0.10     1.00     0.30
     0.00     0.10     0.00     0.30     1.00
 Matrix <i'|x|i'>/<i'|i'>
   0.0000
   0.8670
  -0.8527
   0.0000
   0.0000
 Matrix <i'|y|i'>/<i'|i'>
  -0.0000
  -0.0000
  -0.0488
  -0.4583
   0.4583
 Matrix <i'|z|i'>/<i'|i'>
  -0.1236
   0.5572
   0.5745
  -0.5546
  -0.5546
RANK  5
  15.8482
 Matrix X
     1.00     0.00     0.00     0.00     0.00
     0.00     1.00     0.10     0.10     0.10
     0.00     0.10     1.00     0.10     0.10
```

```
    0.00     0.00     0.10     1.00     0.30
    0.00     0.10     0.10     0.30     1.00
 Matrix <i'|x|i'>/<i'|i'>
   0.0000
   0.8527
  -0.8670
   0.0000
   0.0000
 Matrix <i'|y|i'>/<i'|i'>
  -0.0000
   0.0488
   0.0000
  -0.4583
   0.4583
 Matrix <i'|z|i'>/<i'|i'>
  -0.1236
   0.5745
   0.5572
  -0.5546
  -0.5546
RANK  6
  15.8482
 Matrix X
    1.00     0.00     0.00     0.00     0.00
    0.00     1.00     0.10     0.10     0.10
    0.00     0.10     1.00     0.10     0.10
    0.00     0.10     0.10     1.00     0.30
    0.00     0.00     0.10     0.30     1.00
 Matrix <i'|x|i'>/<i'|i'>
   0.0000
   0.8527
  -0.8670
   0.0000
   0.0000
 Matrix <i'|y|i'>/<i'|i'>
  -0.0000
  -0.0488
```

```
   0.0000
  -0.4583
   0.4583
 Matrix <i'|z|i'>/<i'|i'>
  -0.1236
   0.5745
   0.5572
  -0.5546
  -0.5546
RANK  7
  15.8482
 Matrix X
     1.00     0.00     0.00     0.00     0.00
     0.00     1.00     0.10     0.10     0.10
     0.00     0.10     1.00     0.10     0.10
     0.00     0.10     0.00     1.00     0.30
     0.00     0.10     0.10     0.30     1.00
 Matrix <i'|x|i'>/<i'|i'>
   0.0000
   0.8670
  -0.8527
   0.0000
   0.0000
 Matrix <i'|y|i'>/<i'|i'>
  -0.0000
  -0.0000
   0.0488
  -0.4583
   0.4583
 Matrix <i'|z|i'>/<i'|i'>
  -0.1236
   0.5572
   0.5745
  -0.5546
  -0.5546
RANK  8
  15.8422
```

```
 Matrix X
     1.00     0.00     0.00     0.00     0.00
     0.00     1.00     0.00     0.10     0.10
     0.00     0.00     1.00     0.10     0.10
     0.00     0.10     0.10     1.00     0.30
     0.00     0.10     0.10     0.30     1.00
 Matrix <i'|x|i'>/<i'|i'>
   0.0000
   0.8889
  -0.8889
   0.0000
   0.0000
 Matrix <i'|y|i'>/<i'|i'>
  -0.0000
  -0.0000
   0.0000
  -0.4583
   0.4583
 Matrix <i'|z|i'>/<i'|i'>
  -0.1236
   0.5218
   0.5218
  -0.5546
  -0.5546
RANK  9
  15.8408
 Matrix X
     1.00     0.00     0.00     0.00     0.00
     0.00     1.00     0.10     0.10     0.10
     0.00     0.10     1.00     0.10     0.10
     0.00     0.10     0.00     1.00     0.30
     0.00     0.00     0.10     0.30     1.00
 Matrix <i'|x|i'>/<i'|i'>
   0.0000
   0.8527
  -0.8527
   0.0000
```

```
  0.0000
 Matrix <i'|y|i'>/<i'|i'>
  -0.0000
  -0.0488
   0.0488
  -0.4583
   0.4583
 Matrix <i'|z|i'>/<i'|i'>
  -0.1236
   0.5745
   0.5745
  -0.5546
  -0.5546
RANK 10
  15.8408
 Matrix X
     1.00     0.00     0.00     0.00     0.00
     0.00     1.00     0.10     0.10     0.10
     0.00     0.10     1.00     0.10     0.10
     0.00     0.00     0.10     1.00     0.30
     0.00     0.10     0.00     0.30     1.00
 Matrix <i'|x|i'>/<i'|i'>
   0.0000
   0.8527
  -0.8527
   0.0000
   0.0000
 Matrix <i'|y|i'>/<i'|i'>
  -0.0000
   0.0488
  -0.0488
  -0.4583
   0.4583
 Matrix <i'|z|i'>/<i'|i'>
  -0.1236
   0.5745
   0.5745
```

```
-0.5546
-0.5546
```

Program output for Run 3

```
RANK  1
  17.1854
 Matrix X
     1.00     0.00     0.00     0.00     0.00
     0.00     1.00   -10.00     0.00    10.00
     0.00    10.00     1.00    10.00     0.00
     0.00     1.00    -1.00     1.00     1.00
     0.00     1.00    -1.00     1.00     1.00
 Matrix <i'|x|i'>/<i'|i'>
   0.0000
  -0.8670
   0.8770
  -0.8889
   0.8889
 Matrix <i'|y|i'>/<i'|i'>
  -0.0000
   0.0000
  -0.0000
   0.0000
  -0.0000
 Matrix <i'|z|i'>/<i'|i'>
  -0.1236
   0.5572
   0.4870
   0.5218
   0.5218
RANK  2
  17.1854
 Matrix X
     1.00     0.00     0.00     0.00     0.00
     0.00     1.00   -10.00    10.00     0.00
     0.00    10.00     1.00     0.00    10.00
     0.00     1.00    -1.00     1.00     1.00
     0.00     1.00    -1.00     1.00     1.00
 Matrix <i'|x|i'>/<i'|i'>
   0.0000
```

```
  -0.8670
   0.8770
   0.8889
  -0.8889
 Matrix <i'|y|i'>/<i'|i'>
  -0.0000
   0.0000
  -0.0000
  -0.0000
   0.0000
 Matrix <i'|z|i'>/<i'|i'>
  -0.1236
   0.5572
   0.4870
   0.5218
   0.5218
RANK  3
  17.1854
 Matrix X
     1.00     0.00     0.00     0.00     0.00
     0.00     1.00    10.00     0.00    10.00
     0.00   -10.00     1.00    10.00     0.00
     0.00    -1.00     1.00     1.00     1.00
     0.00    -1.00     1.00     1.00     1.00
 Matrix <i'|x|i'>/<i'|i'>
   0.0000
  -0.8770
   0.8670
  -0.8889
   0.8889
 Matrix <i'|y|i'>/<i'|i'>
  -0.0000
   0.0000
  -0.0000
   0.0000
  -0.0000
 Matrix <i'|z|i'>/<i'|i'>
```

```
  -0.1236
   0.4870
   0.5572
   0.5218
   0.5218
RANK  4
  17.1854
 Matrix X
     1.00     0.00     0.00     0.00     0.00
     0.00     1.00    10.00    10.00     0.00
     0.00   -10.00     1.00     0.00    10.00
     0.00    -1.00     1.00     1.00     1.00
     0.00    -1.00     1.00     1.00     1.00
 Matrix <i'|x|i'>/<i'|i'>
   0.0000
  -0.8770
   0.8670
   0.8889
  -0.8889
 Matrix <i'|y|i'>/<i'|i'>
  -0.0000
   0.0000
  -0.0000
  -0.0000
   0.0000
 Matrix <i'|z|i'>/<i'|i'>
  -0.1236
   0.4870
   0.5572
   0.5218
   0.5218
RANK  5
  17.1838
 Matrix X
     1.00     0.00     0.00     0.00     0.00
     0.00     1.00    10.00     0.00    10.00
     0.00    10.00     1.00    10.00     0.00
```

```
    0.00     1.00     1.00     1.00     1.00
    0.00     1.00     1.00     1.00     1.00
 Matrix <i'|x|i'>/<i'|i'>
   0.0000
  -0.8670
   0.8670
  -0.8889
   0.8889
 Matrix <i'|y|i'>/<i'|i'>
  -0.0000
   0.0000
  -0.0000
   0.0000
  -0.0000
 Matrix <i'|z|i'>/<i'|i'>
  -0.1236
   0.5572
   0.5572
   0.5218
   0.5218
RANK  6
  17.1838
 Matrix X
    1.00     0.00     0.00     0.00     0.00
    0.00     1.00    10.00    10.00     0.00
    0.00    10.00     1.00     0.00    10.00
    0.00     1.00     1.00     1.00     1.00
    0.00     1.00     1.00     1.00     1.00
 Matrix <i'|x|i'>/<i'|i'>
   0.0000
  -0.8670
   0.8670
   0.8889
  -0.8889
 Matrix <i'|y|i'>/<i'|i'>
  -0.0000
   0.0000
```

```
  -0.0000
  -0.0000
   0.0000
 Matrix <i'|z|i'>/<i'|i'>
  -0.1236
   0.5572
   0.5572
   0.5218
   0.5218
RANK  7
  17.1824
 Matrix X
     1.00     0.00     0.00     0.00     0.00
     0.00     1.00    10.00     0.00    10.00
     0.00    -1.00     1.00    10.00     0.50
     0.00   -10.00     0.50     1.00     0.50
     0.00   -10.00     0.50     1.00     1.00
 Matrix <i'|x|i'>/<i'|i'>
   0.0000
  -0.0512
   0.8569
  -0.8889
   0.8766
 Matrix <i'|y|i'>/<i'|i'>
  -0.0000
   0.0000
  -0.0000
   0.0000
   0.0247
 Matrix <i'|z|i'>/<i'|i'>
  -0.1236
  -0.6933
   0.5779
   0.5218
   0.5505
RANK  8
  17.1824
```

```
 Matrix X
     1.00     0.00     0.00     0.00     0.00
     0.00     1.00    10.00    10.00     0.00
     0.00    -1.00     1.00     0.50    10.00
     0.00   -10.00     0.50     1.00     1.00
     0.00   -10.00     0.50     0.50     1.00
 Matrix <i'|x|i'>/<i'|i'>
   0.0000
  -0.0512
   0.8569
   0.8766
  -0.8889
 Matrix <i'|y|i'>/<i'|i'>
  -0.0000
   0.0000
  -0.0000
  -0.0247
   0.0000
 Matrix <i'|z|i'>/<i'|i'>
  -0.1236
  -0.6933
   0.5779
   0.5505
   0.5218
RANK  9
  17.1824
 Matrix X
     1.00     0.00     0.00     0.00     0.00
     0.00     1.00    -1.00    10.00     0.50
     0.00    10.00     1.00     0.00    10.00
     0.00     0.50   -10.00     1.00     0.50
     0.00     0.50   -10.00     1.00     1.00
 Matrix <i'|x|i'>/<i'|i'>
   0.0000
  -0.8569
   0.0512
   0.8889
```

```
 -0.8766
 Matrix <i'|y|i'>/<i'|i'>
 -0.0000
  0.0000
  0.0000
 -0.0000
  0.0247
 Matrix <i'|z|i'>/<i'|i'>
 -0.1236
  0.5779
 -0.6933
  0.5218
  0.5505
RANK 10
 17.1824
 Matrix X
    1.00     0.00     0.00     0.00     0.00
    0.00     1.00    -1.00     0.50    10.00
    0.00    10.00     1.00    10.00     0.00
    0.00     0.50   -10.00     1.00     1.00
    0.00     0.50   -10.00     0.50     1.00
 Matrix <i'|x|i'>/<i'|i'>
  0.0000
 -0.8569
  0.0512
 -0.8766
  0.8889
 Matrix <i'|y|i'>/<i'|i'>
 -0.0000
  0.0000
  0.0000
 -0.0247
 -0.0000
 Matrix <i'|z|i'>/<i'|i'>
 -0.1236
  0.5779
 -0.6933
```

```
0.5505
0.5218
```

B Appendix B

The following is the program used to scan through all possible 5x5 transformation matrices for a set of chosen possible parameter values given that the first orbital is frozen, and there are values of unity along the diagonal. The program begins by inputting all required data including the orthogonal Boys orbital coefficients, overlap integrals for basis functions and one-electron dipole integrals for basis functions. A recursive algorithm is then used as a more flexible alternative to nested loops in order to allow every variational parameter to have each of the chosen possible values in all combinations. The recursive subroutine is called recursive_scan_d which contains a for-loop to go through all the possible parameter values. Upon a modification of the value of one of the variational parameters, the columns are then normalized and the subroutine update_ro recalculates the one-electron dipole integrals and hence centroids for the new orbitals. Afterwards the subroutine calc_boys_func then calculates the value of the Boys sub-functional and compares it to the lowest value in the list of current highest values to determine whether it belongs in this list. The list of highest values achieved throughout the whole program, along with the transformation matrices and dipole integrals associated, is presented after program completion. A series of text files which are numbered from 0 to 9999 are produced in order to inform the user of the degree of completion of the algorithm.

```
      program transformation_scan_program
c-------------------------------------------------------------
c     Boys localization scanning program (PH, September 2016)
c-------------------------------------------------------------
      implicit none
      character*256 percent_thru, results
  logical :: fexist
  real*8, dimension(500) :: c, s, x, y, z, so, xo, yo, zo
  real*8, dimension(25) :: d
      integer, dimension(12) :: cat, a
  real*8, dimension(10,3) :: ro
  integer, dimension(500) :: kw
  real*8, dimension(3) :: diff
  real*8 :: boys_func,
     .         diff_mag, norm2
  integer :: i,k,j,n,m,l,p,norbs, nbas, nbb
  real*8, dimension(9) :: para_values !dimension of this given by para
  integer :: para
```

```
  type optimized_d
real*8 :: boys_func
    real*8, dimension(25) :: d
real*8, dimension(10,3) :: ro
  end type optimized_d
  type(optimized_d), dimension(10) :: max_boys

  !when changed, change the array dimension
  !para_values=(/ -0.7,-0.5,-0.3,-0.1,0.0,0.1,0.3,0.5,0.7 /)
  !para_values=(/ -5.0,-1.0,-0.5,-0.25,0.0,0.25,0.5,1.0,5.0 /)
  !para_values=(/ -1.0,-0.5,-0.25,0.0,0.25,0.5,1.0 /)
  para_values=(/ -10.0,-5.0,-1.0,-0.5,0.0,0.5,1.0,5.0,10.0 /)
  para = 9
  a =(/ 8,9,10, 12,14,15, 17,18,20, 22,23,24 /)



 !The program inputs a file called 'gamess_boys.txt', this is a file with a personal
 !standard format of GAMESS
   !data produced in one of our programs for the orthogonal boys procedure.
   !From the way this program reads
   !this file, it is possible to deduce the format of this file.

  !d is the 5x5 transformation matrix (from the Boys orbital basis)
  !only the latter 4x4 section has any varied parameters
  !diagonal elements of d are fixed at 1
  !initialize the transformation matrix to be the identity matrix
  do i=1,5
do j=1,5
if(i.eq.j)then
   d((i-1)*5+j) = 1d0
else
   d((i-1)*5+j) = 0d0
endif
enddo
  enddo

  write(*,
```

```
     .'(''Scan through possible transformation matrices''/
     .  ''-------------------------------------------------'')')

 !Read in MO data
      open(unit=106, file='gamess_boys.txt')
  read(106,*) norbs, nbas
  nbb = nbas*(nbas + 1)/2
  read(106,*) (c(i), i=1,norbs*nbas)
  read(106,*) (s(i), i=1,nbb)
  read(106,*) (x(i), i=1,nbb)
  read(106,*) (y(i), i=1,nbb)
  read(106,*) (z(i), i=1,nbb)
  close(106)

  !Progress check produces files from 0.txt up to 9999.txt,
  !representing program completion
  percent_thru = '0.txt'
  inquire(file = percent_thru, exist = fexist)
  if(fexist)then
open(unit=107, file=percent_thru, status='old')
close(107,status='delete')
  endif
  open(unit=107, file=percent_thru, status='new')

      kw(1) = 0
      do i = 2, nbas
        kw(i) = kw(i - 1) + i - 1
      enddo
  call tr1e(nbas, norbs, x, xo, c, kw)
  call tr1e(nbas, norbs, y, yo, c, kw)
  call tr1e(nbas, norbs, z, zo, c, kw)
  !xo, yo, zo now contain the (dipole) matrix elements of x,y,z in the boys orbital

  do l=1,10
    max_boys(l)%boys_func = 5d0 - l*0.01d0
  enddo
  do l=1,12
```

```
    cat(l) = 1
!one value for each variational matrix element
!algorithm starts at 1 1 1 ... 1, ends in para para para ... para.
!cat gives the values from para_values which each matrix element will take
  enddo
  do k=1,12
d(a(k)) = para_values(cat(k))
  enddo
  do l=1,5
     call update_ro(l) !get ro fully initialized ready to tweak individual
     !elements throughout program
  enddo

  !begin algorithm
  call recursive_scan_d(1)

  !the algorithm has now finished
  close(107,status='delete')
  results = 'results.txt'
  inquire(file = results, exist = fexist)
  if(fexist)then
open(unit=107, file=results, status='old')
close(107,status='delete')
  endif
  open(unit=107, file=results, status='new')

  do n=1,10
write(107,'(A,I2)') 'RANK ', n
write(107,'(F9.4)') max_boys(n)%boys_func
write(107,*) 'Matrix X'
do l = 1, 5
  write(107,'(5F9.2)') (max_boys(n)%d((k-1)*5+l), k=1,5)
enddo
write(107,*) 'Matrix <i''|x|i''>/<i''|i''>'
do l = 1, 5
      write(107,'(F9.4)') max_boys(n)%ro(l,1)
enddo
```

```
write(107,*) 'Matrix <i''|y|i''>/<i''|i''>'
do l = 1, 5
      write(107,'(F9.4)') max_boys(n)%ro(l,2)
enddo
write(107,*) 'Matrix <i''|z|i''>/<i''|i''>'
do l = 1, 5
      write(107,'(F9.4)') max_boys(n)%ro(l,3)
enddo
  enddo

  close(107)

  write(6,*) 'All Done'

  contains
    recursive subroutine recursive_scan_d(j) !j identifies the element being tweaked
      integer j, i, points_thru

      do i=1,para !one cycle for each member of para_values
    if(j.lt.12)then
  !if not at the deepest level, go deeper
      call recursive_scan_d(j+1)
if(j.eq.5)then  !PROGRESS CHECK : happens roughly every 5.4sec
  !Give feedback on progress
  close(107,status='delete')
         points_thru = 0
  do l=1,5
       points_thru = points_thru + (cat(l)-1)*para**(5-l)
  enddo
  points_thru = Int(100*100*points_thru/para**5)
         write(percent_thru,'(I5,A)')points_thru,'.txt'
         !goes to 10,000
  open(unit=107, file=percent_thru, status='new')

endif
    endif
    if(i.ne.para)then !the final increment won't have a chance to scan lower levels
```

```
      cat(j) = cat(j) + 1
  d(a(j)) = para_values(cat(j)) !every time cat changes, update d
  !now update only the diagonal element of ro which will be affected
  call update_ro(Int((j-1)/3d0) + 2)
  !this is the MO corresponding to j
  !only check boys func if an increment has been made (at any level)
  call calc_boys_func()
    else
      cat(j) = 1
  d(a(j)) = para_values(cat(j)) !every time cat changes, update d
  !now update only the diagonal element of ro which will be affected
  call update_ro(Int((j-1)/3d0) + 2)
  !this is the MO corresponding to j
    endif
  enddo
    end subroutine

subroutine update_ro(k)
  integer k, starter
      ro(k,1) = 0d0
      ro(k,2) = 0d0
      ro(k,3) = 0d0
  if(k.eq.1)then !a further efficiency enhancer
starter = 1
  else
    starter = 2
  endif
      do n=starter,norbs
    do m=starter,norbs
      if(n.le.m)then
    ro(k,1)= ro(k,1) + d((k-1)*5+n)*d((k-1)*5+m)*xo((m-1)*m/2+n)
ro(k,2)= ro(k,2) + d((k-1)*5+n)*d((k-1)*5+m)*yo((m-1)*m/2+n)
ro(k,3)= ro(k,3) + d((k-1)*5+n)*d((k-1)*5+m)*zo((m-1)*m/2+n)
      else
    ro(k,1)= ro(k,1) + d((k-1)*5+n)*d((k-1)*5+m)*xo((n-1)*n/2+m)
ro(k,2)= ro(k,2) + d((k-1)*5+n)*d((k-1)*5+m)*yo((n-1)*n/2+m)
ro(k,3)= ro(k,3) + d((k-1)*5+n)*d((k-1)*5+m)*zo((n-1)*n/2+m)
```

```
      endif
    enddo
      enddo
      norm2 = 0d0
      do n=1,norbs
    !boys orbitals are orthogonal, hence norm is the sum of squares of column elemen
    norm2 = norm2 + d((k-1)*5+n)**2
      enddo
      ro(k,1) = ro(k,1)/norm2
      ro(k,2) = ro(k,2)/norm2
      ro(k,3) = ro(k,3)/norm2
      !Therefore now ro(k,1) == <k'|x|k'>/<k'|k'>
end subroutine

      subroutine calc_boys_func()
   !ro(k) = <k'|r|k'>/<k'|k'>, now assimilate these
   boys_func = 0d0
       do n=1,norbs
         do m=n+1,norbs
           diff_mag = 0d0
       do l=1,3
             diff(l) = ro(n,l)-ro(m,l)
         diff_mag = diff_mag + diff(l)**2
           enddo
       boys_func = boys_func + diff_mag
         enddo
       enddo

       if(boys_func.gt.max_boys(10)%boys_func)then !entry 10 smallest
l=1
    do while(l.le.10)
  if(boys_func.gt.max_boys(l)%boys_func)then
    if(l.lt.10)then
      do n=10,l+1,-1
    !max_boys_func(n) = max_boys_func(n-1)
max_boys(n) = max_boys(n-1)
  enddo
```

```
endif
max_boys(l)%boys_func = boys_func
max_boys(l)%d = d
max_boys(l)%ro = ro
l=999
  endif
  l = l+1
enddo
        endif
    end subroutine
      end program transformation_scan_program



      subroutine tr1e(nbas, norbs, a, ao, c, kw)
c---- Transforms a one-electron operator from AO (a) to MO (ao) basis.
c     (PBK, April 2016)
c-------------------------------------------------------------
      implicit real*8 (a-h, o-z)
      dimension kw(*), a(*), ao(*), c(*), v(nbas)

      ij = 0
      do 50 j = 1, norbs
        jofs = (j - 1)*nbas
        do 20 k = 1, nbas
          vk = 0d0
          kwk = kw(k)

          do 11 l = 1, k
            vk = vk + a(l + kwk)*c(jofs + l)
   11     continue

          do 12 l = k + 1, nbas
            vk = vk + a(k + kw(l))*c(jofs + l)
   12     continue
          v(k) = vk
   20   continue
        do 40 i = 1, j
```

```
            ij = ij + 1
            iofs = (i - 1)*nbas
            aoij = 0d0
            do 30 k = 1, nbas
   30         aoij = aoij + c(iofs + k)*v(k)
              ao(ij) = aoij
   40     continue
   50   continue
        return
        end
c-------------------------------------------------------------------------
```

References

[1] HO Pritchard and FH Sumner. The calculation of bond lengths in naphthalene and anthracene. *Transactions of the Faraday Society*, 51(4):457–462, 1955.

[2] ZF Chen, CS Wannere, C Corminboeuf, R Puchta, and PV Schleyer. Nucleus-independent chemical shifts (nics) as an aromaticity criterion. *Chemical Reviews*, 105(10):3842–3888, 2005.

[3] PV Schleyer, C Maerker, A Dransfeld, HJ Jiao, and NJRV Hommes. Nucleus-independent chemical shifts: A simple and efficient aromaticity probe. *Journal of the American Chemical Society*, 118(26):6317–6318, 1996.

[4] PV Schleyer, M Manoharan, ZX Wang, B Kiran, HJ Jiao, R Puchta, and NJRV Hommes. Dissected nucleus-independent chemical shift analysis of pi-aromaticity and antiaromaticity. *Organic Letters*, 3(16):2465–2468, 2001.

[5] Peter B. Karadakov, Peter Hearnshaw, and Kate E. Horner. Magnetic shielding, aromaticity, antiaromaticity, and bonding in the low-lying electronic states of benzene and cyclobutadiene. *The Journal of Organic Chemistry*, 81(22):11346–11352, 2016.

[6] R. Shankar. *Principles of Quantum Mechanics*. Springer, seconds edition, 2010.

[7] R. McWeeny. *Methods of Molecular Quantum Mechanics*. Academic Press, second edition, 1992.

[8] Attila Szabo and Neil S. Ostlund. *Modern Quantum Chemistry*. McGraw-Hill Publishing Company, first edition, revised edition, 1996.

[9] R. Islas, E. Chamorro, J. Robles, T. Heine, J. C. Santos, and G. Merino. Borazine: to be or not to be aromatic. *Structural Chemistry*, 18(6):833–839, 2007.

[10] I. Alkorta, I. Rozas, and J. Elguero. An ab initio study of the nmr properties (absolute shieldings and nics) of a series of significant aromatic and antiaromatic compounds. *Tetrahedron*, 57(28):6043–6049, 2001.

[11] O. P. Charkin, N. M. Klimenko, D. Moran, A. M. Mebe, D. O. Charkin, and P. V. Schleyer. Theoretical study of icosahedral closo-borane, -alane, and -gallane dianions (a(12)h(12)(2-); a = b, al, ga) with endohedral noble gas atoms (ng = he, ne, ar, and kr) and their lithium salts (li ng@a(12)h(12) (-) and li-2 ng@a(12)h(12)). *Inorganic Chemistry*, 40(27):6913–6922, 2001.

[12] D. Delaere, M. T. Nguyen, and L. G. Vanquickenborne. A theoretical study on the molecular and electronic structure of heteroaromatic bowl-shaped molecules. *Chemical Physics Letters*, 333(1-2):103–112, 2001.

[13] L. A. Paquette, W. Bauer, M. R. Sivik, M. Buhl, M. Feigel, and P. V. Schleyer. Structure of lithium isodicyclopentadienide and lithium cyclopentadienide in tetrahydrofuran solution - a combined nmr, iglo, and mndo study. *Journal of the American Chemical Society*, 112(24):8776–8789, 1990.

[14] C. M. Stanisky, R. J. Cross, and M. Saunders. Putting atoms and molecules into chemically opened fullerenes. *Journal of the American Chemical Society*, 131(9):3392–3395, 2009.

[15] M. Buhl and A. Hirsch. Spherical aromaticity of fullerenes. *Chemical Reviews*, 101(5):1153–1183, 2001.

[16] P. V. Schleyer, H. J. Jiao, Njrv Hommes, V. G. Malkin, and O. L. Malkina. An evaluation of the aromaticity of inorganic rings: Refined evidence from magnetic properties. *Journal of the American Chemical Society*, 119(51):12669–12670, 1997.

[17] J. Pipek and P. G. Mezey. A fast intrinsic localization procedure applicable for abinitio and semiempirical linear combination of atomic orbital wave-functions. *Journal of Chemical Physics*, 90(9):4916–4926, 1989.

[18] S. F. Boys. Construction of some molecular orbitals to be approximately invariant for changes from one molecule to another. *Reviews of Modern Physics*, 32(2):296–299, 1960.

[19] H Fallah-Bagher-Shaidaei, CS Wannere, C Corminboeuf, R Puchta, and PV Schleyer. Which nics aromaticity index for planar pi rings is best? *Organic Letters*, 8(5):863–866, 2006.

[20] K. Wolinski. Magnetic shielding surface in molecules. neutron as a probe in the hypothetical magnetic resonance spectroscopy. *Journal of Chemical Physics*, 106(14):6061–6067, 1997.

[21] C. E. Johnson and F. A. Bovey. Calculation of nuclear magnetic resonance spectra of aromatic hydrocarbons. *Journal of Chemical Physics*, 29(5):1012–1014, 1958.

[22] S. Klod and E. Kleinpeter. Ab initio calculation of the anisotropy effect of multiple bonds and the ring current effect of arenes - application in conformational and configurational analysis. *Journal of the Chemical Society-Perkin Transactions 2*, (10):1893–1898, 2001.

[23] S. Klod, A. Koch, and E. Kleinpeter. Ab-initio quantum-mechanical giao calculation of the anisotropic effect of c-c and x-c single bonds - application to the h-1 nmr spectrum of cyclohexane. *Journal of the Chemical Society-Perkin Transactions 2*, (9):1506–1509, 2002.

[24] E. Kleinpeter, S. Klod, and A. Koch. Visualization of through space nmr shieldings of aromatic and anti-aromatic molecules and a simple means to compare and estimate aromaticity. *Journal of Molecular Structure-Theochem*, 811(1-3):45–60, 2007.

[25] PB Karadakov and KE Horner. Magnetic shielding in and around benzene and cyclobutadiene: A source of information about aromaticity, antiaromaticity, and chemical bonding. *Journal of Physical Chemistry a*, 117(2):518–523, 2013.

[26] KE Homer and PB Karadakov. Chemical bonding and aromaticity in furan, pyrrole, and thiophene: A magnetic shielding study. *Journal of Organic Chemistry*, 78(16):8037–8043, 2013.

[27] PB Karadakov and KE Horner. Exploring chemical bonds through variations in magnetic shielding. *Journal of Chemical Theory and Computation*, 12(2):558–563, 2016.

[28] RFW Bader. Atoms in molecules. *Accounts of Chemical Research*, 18(1):9–15, 1985.

[29] PB Karadakov. Ground- and excited-state aromaticity and antiaromaticity in benzene and cyclobutadiene. *Journal of Physical Chemistry a*, 112(31):7303–7309, 2008.

[30] PB Karadakov. Aromaticity and antiaromaticity in the low-lying electronic states of cyclooctatetraene. *Journal of Physical Chemistry a*, 112(49):12707–12713, 2008.

[31] M. Kataoka. Magnetic susceptibility and aromaticity in the excited states of benzene. *Journal of Chemical Research-S*, (8):573–574, 2004.

[32] NC Baird. Quantum organic photochemistry .2. resonance and aromaticity in lowest pi-3-pi] state of cyclic hydrocarbons. *Journal of the American Chemical Society*, 94(14):4941, 1972.

[33] WJ Buma, JH Vanderwaals, and MC Vanhemert. Conformational instability of the lowest triplet-state of the benzene nucleus .1. the unsubstituted molecule. *Journal of Chemical Physics*, 93(6):3733–3745, 1990.

[34] A. Soncini and P. W. Fowler. Ring-current aromaticity in open-shell systems. *Chemical Physics Letters*, 450(4-6):431–436, 2008.

[35] F. Fratev, V. Monev, and R. Janoschek. Abinitio study of cyclobutadiene in excited-states - optimized geometries, electronic-transitions and aromaticities. *Tetrahedron*, 38(19):2929–2932, 1982.

[36] A. Minsky, A. Y. Meyer, and M. Rabinovitz. Paratropicity and antiaromaticity - role of the homo lumo energy-gap. *Tetrahedron*, 41(4):785–791, 1985.

[37] J. A. Pople. Proton magnetic resonance of hydrocarbons. *Journal of Chemical Physics*, 24(5):1111–1111, 1956.

[38] J. S. Waugh and R. W. Fessenden. Nuclear resonance spectra of hydrocarbons - the free electron model. *Journal of the American Chemical Society*, 79(4):846–849, 1957.

[39] CS Wannere and PV Schleyer. How do ring currents affect h-1 nmr chemical shifts? *Organic Letters*, 5(5):605–608, 2003.

[40] K. Aidas, C. Angeli, K. L. Bak, V. Bakken, R. Bast, L. Boman, O. Christiansen, R. Cimiraglia, S. Coriani, P. Dahle, E. K. Dalskov, U. Ekstrom, T. Enevoldsen, J. J. Eriksen, P. Ettenhuber, B. Fernandez, L. Ferrighi, H. Fliegl, L. Frediani, K. Hald, A. Halkier, C. Hattig, H. Heiberg, T. Helgaker, A. C. Hennum, H. Hettema, E. Hjertenaes, S. Host, I. M. Hoyvik, M. F. Iozzi, B. Jansik, H. J. A. Jensen, D. Jonsson, P. Jorgensen, J. Kauczor, S. Kirpekar, T. Kjrgaard, W. Klopper, S. Knecht, R. Kobayashi, H. Koch, J. Kongsted, A. Krapp, K. Kristensen, A. Ligabue, O. B. Lutnaes, J. I. Melo, K. V. Mikkelsen, R. H. Myhre, C. Neiss, C. B. Nielsen, P. Norman, J. Olsen, J. M. H. Olsen, A. Osted, M. J. Packer, F. Pawlowski, T. B. Pedersen, P. F. Provasi, S. Reine, Z. Rinkevicius, T. A. Ruden, K. Ruud, V. V. Rybkin, P. Salek, C. C. M. Samson, A. S. de Meras, T. Saue, S. P. A. Sauer, B. Schimmelpfennig, K. Sneskov, A. H. Steindal, K. O. Sylvester-Hvid, P. R. Taylor, A. M. Teale, E. I. Tellgren, D. P. Tew, A. J. Thorvaldsen, L. Thogersen, O. Vahtras, M. A. Watson, D. J. D. Wilson, M. Ziolkowski, and H. Agren. The dalton quantum chemistry program system. *Wiley Interdisciplinary Reviews-Computational Molecular Science*, 4(3):269–284, 2014.

[41] K. Ruud, T. Helgaker, R. Kobayashi, P. Jorgensen, K. L. Bak, and H. J. A. Jensen. Multiconfigurational self-consistent-field calculations of nuclear shieldings using london atomic orbitals. *Journal of Chemical Physics*, 100(11):8178–8185, 1994.

[42] K. Ruud, T. Helgaker, K. L. Bak, P. Jorgensen, and J. Olsen. Accurate magnetizabilities of the isoelectronic series beh-, bh, and ch+ - the mcscf-giao approach. *Chemical Physics*, 195(1-3):157–169, 1995.

[43] P.W. Atkins and R.S. Friedman. *Molecular Quantum Mechanics*. Oxford University Press, third edition edition, 1997.

[44] J. Gerratt, D. L. Cooper, P. B. Karadakov, and M. Raimondi. Modern valence bond theory. *Chemical Society Reviews*, 26(2):87–100, 1997.

[45] C. Edmiston and K. Ruedenberg. Localized atomic and molecular orbitals. *Reviews of Modern Physics*, 35(3):457, 1963.

[46] C. Edmiston and K. Ruedenberg. Localized atomic and molecular orbitals . 2. *Journal of Chemical Physics*, 43(10):S097–+, 1965.

Bibliography

[1] P.W. Atkins and R.S. Friedman. *Molecular Quantum Mechanics*. Oxford University Press, third edition, 1997.

[2] R. Shankar. *Principles of Quantum Mechanics*. Springer, second edition, 2010.

[3] R. McWeeny. *Methods of Molecular Quantum Mechanics*. Academic Press, second edition, 1992.

[4] Peter B. Karadakov, Peter Hearnshaw, and Kate E. Horner. Magnetic shielding, aromaticity, antiaromaticity, and bonding in the low-lying electronic states of benzene and cyclobutadiene. *The Journal of Organic Chemistry*, 81(22):11346–11352, 2016.

[5] Attila Szabo and Neil S. Ostlund. *Modern Quantum Chemistry*. McGraw-Hill Publishing Company, first edition, revised edition, 1996.

[6] J. Pipek and P. G. Mezey. A fast intrinsic localization procedure applicable for abinitio and semiempirical linear combination of atomic orbital wave-functions. *Journal of Chemical Physics*, 90(9):4916–4926, 1989.

[7] R Gershoni-Poranne and A Stanger. Magnetic criteria of aromaticity. *Chemical Society Reviews*, 44(18):6597–6615, 2015.